Mixed Methods and Reduced Integration for the Circular Arch Problem

M B Volpi

March 23, 1991

Abstract

The boundary-value problem for linear elastic circular arches is studied. The governing equations are based on the Timoshenko-Reissner-Mindlin hypotheses. The problem is formulated in both the standard and mixed variational forms which include a parameter relating to the thickness of the arch. Existence and uniqueness of solutions to these equivalent problems is established and the corresponding discrete problems are studied. Finite element approximations to the mixed problem are shown to be stable and convergent, and selective reduced integration applied to the standard discrete problem renders it equivalent to the mixed problem. The results of numerical experiments are presented; these confirm the convergent behaviour of the mixed problem. For the standard problem with full integration convergence is suboptimal or nonexistent for small values of the thickness parameter, while for the mixed or selectively reduced integration problem the numerical rates of convergence coincide with those predicted by the theory.

To my parents

Thank you for your love and support.

Contents

List of Figures

1 Introduction

Beams (that is, straight bars subject to transverse loading), circular beams (that is, arches), plates and shells are the basic structural elements in many engineering structures such as ship hulls, wings and fuselages of aircraft, automobile tyres, concrete dam walls and many other structures. A great deal of research has therefore gone into the formulation and analysis of mathematical models for these basic structures [2] [6]. These mathematical models are obtained by making simplifying assumptions about the geometry, kinematics and stress fields in a continuous medium.

Much work has been done on the formulation of finite elements for curved beams [6] [42] [41] [29] [44]. One reason for their importance is that they are useful for a variety of engineering applications, for example arch-like structures, pipelines and rings. More importantly, much can be learned from studying the essentially one dimensional curved beam models, so as to gain insight into the behaviour of more complex two-dimensional shell models. Many of the problems that exist in finite element analyses of shell problems, for example stretching-flexural interaction, inabilities in representing rigid body motion and shear and membrane locking, exhibit themselves in curved beam analysis. Assemblages of flat plates have also been used for the analysis of shells [2], but with limited success compared to the circular beam. One reason for their limited success is that, whereas membrane (bending) deformation exists throughout the circular arch, it is restricted to the couplings between plates in plate assemblages. Also, curved elements eliminate "discontinuity" moments that plague plate assemblages.

There are basically three approaches that may be used for the formulation of curved elements (curved beams, shells etc.), depending on the theories chosen to derive the underlying governing equations [2]. The first is based on the use of the so-called *intrinsic curved* elements,

where the governing equations are developed in a curvilinear coordinate system and, the exact strain-displacement relationships for deep-arch theories are employed. This has been the most popular approach for arch elements thus far [13] [26] [44] and is the approach we employ for this formulation. The second approach employs "simplified" strain-displacement expressions based on theories for *shallow-arch* type structures [14] [41] [42] [43]. In the third approach, *degenerate continuum* elements are used in which isoparametric representation is used and the general continuum theory is reduced to a curved beam theory by applying appropriate physical and kinematic constraints simultaneously with the finite element discretization [24] [12]. This approach is attractive in that it avoids the mathematical complications associated with the assumptions made in curved element theories. Nevertheless most studies of curved elements, so far, have used one of the first two approaches. This is due mainly to the simplicity of the resulting equations and the ease with which they can be interpreted and assessed.

These one- or two-dimensional problems generally contain complex systems of differential equations and hence, at present, are difficult to solve analytically. A great deal of time has therefore been devoted in recent years to the development of approximate solution methods by finite elements. The finite element method came to fruition in the 1960's and is presently the most powerful and widely used approach for the design and analysis of such structures. The most common variational formulation of problems in the case of beams, arches, plates and shells uses the Kirchhoff-Poisson-Love or Timoshenko-Reissner-Mindlin hypotheses, and is based on the principle of minimal potential energy. This formulation, known as the *displacement* or stiffness method, is favoured for its computational ease and simplicity.

The *Kirchhoff hypothesis* states that plane sections initially normal to the midsurface remain plane and normal to the midsurface after bending. This is known as the Love and Poisson hypotheses for shell and plate theories respectively and amounts to the neglecting of shear

strains. An advantage of the Kirchhoff theory is that the only variables needed in the mathematical formulation are those used to describe the midsurface displacements. Boundary value problems based on this classical theory involve ordinary or partial derivatives of up to fourth order. Therefore displacement-based variational formulations contain derivatives up to second order and hence C^1 continuity is required to ensure interelement compatibility. This is disadvantageous as additional effort is needed to devise element interpolatory schemes which satisfy this condition. Nevertheless, quite a number of such schemes have been developed which, although they involve quite sophisticated, high order interpolation schemes, are set on a firm mathematical basis. See [6] for a summary of convergence results for elements based on the C^1 approach to Kirchhoff theory. Another disadvantage of the Kirchhoff theory is that, because it neglects shear strain, only thin elements, where the span to thickness ratio is small, can be modelled accurately.

Much recent research has therefore taken as a basic assumption the *Timoshenko-Reissner-Mindlin* hypotheses [42] [35] [13] [41] which state that plane sections, initially plane and normal to the centreline, remain plane but not necessarily normal after deformation. Variational formulations based on the Timoshenko theory involve derivatives up to only first order and hence only C^0 interelement continuity is required of the solution. That is, only the generalised displacement degrees of freedom (not their derivatives) must be continuous across element boundaries. Such continuity is easily attained, allowing for the use of low order interpolation functions for approximating the displacement components. From an engineering point of view, these hypotheses are more realistic as shear deformation is incorporated, allowing for the modelling of thick elements.

Despite a seemingly ideal suitability of Timoshenko theory for the development of simple, cost-effective displacement models, the straightforward implementation of low order interpolation functions, using exact integration of element energies, often gives inaccurate results for

thin structures. This phenomenon, where the accuracy of such finite element displacement models rapidly degenerates as the arch becomes thinner is now known as *locking* and arises from the so-called penalty strains [32] [46] [4] (as various penalty type methods are used to inhibit them). These penalty strains arise from the shear strain and, in curved members, the axial (membrane) strain, and cause what is now commonly known as shear and membrane locking, respectively.

Shear locking was first identified by Zienkiewicz and Hinton [47]. Based upon a penalty function formulation of the equations of plate bending they showed that, as the span to thickness ratio of a plate tends towards infinity, a constraint condition is imposed, requiring the product of the shear stiffness matrix and the displacement vector to be zero. Hence the shear stiffness matrix must be singular in order to obtain a non-trivial solution. Alternatively, they suggested that locking was due to the fact that too many independent constraints are imposed on each element compared to the average number of unconstrained degrees of freedom in an assembled mesh. This led to the development of a constraint index by Hughes and his colleagues [31] [32] to predict locking in various finite element meshes. The actual origin of the excess stiffness in shear deformable elements was also clarified by Prathap and Bhashyam [39]. They noted that the singularity of the shear stiffness matrix, or the number of constraints in an element, are not sufficient criteria to completely describe the locking phenomenon. Rather, locking was shown to be a function of the type of constraints that arise in a very thin element. By analysing the exact integration of a Timoshenko beam element they were able to identify the actual constraints that arise under full integration of the shear term and, by deriving the constraints in terms of nodal degrees of freedom, were able to classify them as either true Kirchhoff constraints, or *spurious* constraints that cause locking. They observed that the spurious constraints that arise in thin Timoshenko beam elements are due to a difference in the order of interpolation used for the rotation degrees of

freedom and the derivatives of the transverse displacement. See chapter 4 for a discussion on the true and spurious constraints that arise for the discrete standard variational formulation for the arch using exact integration.

Initially it was thought that the occurrence of membrane locking in thin curved structures, when using low-order independent, polynomial interpolations, was due to the fact that these low-order functions could not represent rigid-body motions explicitly [35] [14]. Hence these simple functions were modified with the inclusion of trigonometric terms which were meant to improve the strain-free, rigid-body modes, and success was achieved [14] [2, chap.6]. Meck [33] showed that membrane locking was not due to the neglect of rigid-body motions, but rather due to the neglect of the coupling required between normal and tangential displacements for the inextensibility condition. Independently, Stolarski and Belytschko [42] and Prathap and Bashyam [39] showed that when low order interpolations are used in approximating the axial term, the inconsistency in the order of the interpolation functions (ie. shape functions) for the variables in the extensional strain energy functional, produces spurious constraints, in the penalty limit of extreme thinness (ie. nearly inextensional behaviour), which are the actual cause of locking. Later Prathap [40] showed that the success of the trigonometric terms defined above was due not to their ability to represent rigid-body motion but rather because they did not exhibit any spurious constraints.

Since the 1970's, most research on arches and related topics has aimed at developing methods which eliminate locking in the Timoshenko-type formulations. One alternative is to use displacement polynomial approximations of sufficiently high order in the finite element model. For example, the quintic-quintic element models of Dawe [2] proved successful for quite a range of shallow and deep arch and shell models [22]. However, difficulties are often encountered, particularly in shell theory, in interpreting the boundary conditions and nodal loads [2] [5].

Others have resorted to modified formulations of the locking-free Kirchhoff theory in which one or both of the main disadvantages discussed earlier are removed. For example, the *discrete Kirchhoff method* [16] [17] [27] (used mainly in plate and shell theory) in which the rotation(s) and normal displacement are treated independently and only C^0 continuity requirements need to be satisfied. The transverse shear term is ignored in the calculation of the stiffness matrix and the errors, due to this approximation, are compensated for by imposing the Kirchhoff constraints along the boundaries. This method, however, makes use of incompatible elements and is restricted only to the modelling of thin structures. Ortiz and Morris [37] derive an alternative formulation for the Kirchhoff's equations for plate theory. In this formulation the potential energy of the plate is formulated entirely in terms of rotations, whereas the displacements are the outcome of a subsidiary problem. The nature of the resulting equations requires only C^0 continuity for the interpolation functions. Since the approach uses Kirchhoff's equations, locking-free results are obtained but the formulation is limited to thin structures.

One popular approach is to adopt an alternative variational formulation to the displacement model, namely the mixed formulation, where one uses simultaneous approximations for both the stresses and the displacements [42] [32] [26] [41]. Here the internal forces appear as Lagrange multipliers, while the displacements are the primal variables. By carefully selecting appropriate parameters for the Lagrange multiplier space and the primal space, it is possible to develop an effective finite element that avoids locking. In Hybrid-mixed formulations [35] [44] [38] the Lagrange multipliers are used to impose the continuity conditions between interelement boundaries. Saleeb and Chang [44] develop guidelines or criteria for choosing suitable parameters in the assumed fields using the constraint index previously introduced by Malkus and Hughes [32]. The earlier applications of mixed finite element methods date as far back as the mid-1960's when they were used to model plate bending by Herrmann

[30]. It was only in the early 1970's though, that the mathematical framework for this theory was established by Brezzi [18] [19] and Babuska [15]. There are however, two disadvantages to these mixed variational type problems as discussed by Malkus and Hughes [32]. Firstly, additional computation is required due to the auxiliary field in the mixed formulation and secondly, the generalisation to non-linear problems is not always apparent.

The most popular method of overcoming locking is via *selective-reduced integration* in which selective terms (namely the penalty terms) of the discrete displacement formulation are underintegrated. That is, Gaussian quadrature of one order less than that required to integrate these terms exactly, is applied. The first example of a reduced integration element was apparently the plate/shell analysis presented by Zienkiewicz, Taylor and Too [48]. A 2×2 Gauss quadrature rule was used on an eight-noded element, instead of the 3×3 Gauss rule required for exact integration of this element, and a considerable improvement was observed. Much research has been done in an attempt to explain how selective-reduced integration is capable of eliminating the locking phenomena [43] [39] [26]. Zienkiewicz was the first to present a detailed reasoning on why reduced integration could alleviate the shear locking phenomenon [12]. Based on his idea that locking was due to the nonsingularity of the stiffness matrix, he showed that reduced integration could make the shear stiffness matrix singular, hence removing the constraint imposed by the shear strain as the thickness became very small. In their analysis of the Timoshenko beam and shallow beam problems, Prathap and Bashyam [39] showed that the spurious constraints, that originate under exact integration of the shear and axial terms, do not appear when reduced integration is used. It was only in 1978 however, that a true mathematical explanation of the ability for selective-reduced integration to alleviate locking could be given. In their paper, Malkus and Hughes established the equivalence of certain classes of mixed finite element methods with the computationally simpler displacement formulations in which selective-reduced integration is employed. This meant

that the existence and convergence theory of the reduced standard problem could be established (a priori) using the firm mathematical foundations of an equivalent mixed formulation.

The methods of selective reduced integration and, in particular, mixed methods have been used in the analysis of two-dimensional structures [20] [46] where the locking phenomena are more complex.

In his analysis of the Timoshenko beam problem, Arnold [13] introduces the thickness of the beam as a parameter which appears in the shear term of the displacement formulation. Error estimates are then derived showing that, finite element approximations to the standard problem are dependent on the thickness parameter and degenerates as the thickness decreases. Using the theory of Brezzi [18] he establishes a mixed formulation which converges at a rate independent of the thickness parameter; he also shows that this discrete mixed problem is equivalent to the discrete standard problem where the shear term has been underintegrated.

Using a similar approach to that of Arnold, Kikuchi [26] analyses the circular arch problem without shear deformation. Expressing the thickness of the arch in a parametric form, he derives a priori error estimates and shows that locking occurs when low-order interpolations are used in the standard discretisation, but not in the class of mixed models that he considers.

The first attempt at analysing a system with two potential sources of locking was apparently that of Loula *et al* [29], who considered the circular arch problem with axial and shear deformation. They constructed convergent finite element approximations for a mixed method based on the Hellinger-Reissner formulation, using a nonstandard Petrov-Galerkin method. The method, which finds its origin and most frequent use in problems of convection and

diffusion, had previously been applied to the beam problem [28]. Loula *et al* analysed a circular arch fixed at one end and free at the other. They found that it was not possible to obtain convergence results for the standard homogeneous Dirichlet problem in which the arch is fixed at both ends; their numerical experiments, however, appeared to indicate that their results carried over to this case as well.

Using a standard mixed formulation Reddy [41] investigated the existence of convergent finite element methods for the shallow arch problem; here there is also the presence of both shear and axial terms. A standard mixed formulation was used, and gave convergent approximations. Equivalence between the mixed method and a selective reduced integration formulation was verified, though only for the case in which the degree s of polynomial approximation of the arch shape satisfies $1 \leq s \leq \min\{2, r\}$, r being the order of polynomial approximation of the displacements and rotation.

Based on the Timoshenko-Reissner-Mindlin theory we develop, in chapter 2, the governing equations for a circular arch with axial and shear deformation. From these governing equations we formulate the variational standard problem, expressing the thickness of the arch through a parameter d, and prove the existence of a unique solution to this problem. An equivalent mixed formulation is derived and the existence of a unique solution is verified, with the use of the Brezzi conditions [18], appropriately generalised to the case $d \in [0, 1]$ in [13]. In chapter 3 we consider the finite element approximations to the standard and mixed formulations. We show that the discrete standard and mixed formulations are not equivalent and that unique, stable and convergent solutions exist to the discrete mixed problem, for sufficiently small values of the mesh parameter. We analyse the causes of locking in the discrete standard problem and then show the equivalence between the reduced standard problem (where the shear and axial terms are underintegrated) and the discrete mixed formulation. Finally, in chapter 4 some numerical results are presented confirming the locking

phenomena in the standard finite element approximation with full integration, and the good convergence rates in the case of the discrete mixed or reduced standard formulations.

2 The Continuous Problem

In this section we derive the governing equations for the circular arch subject to the Timoshenko hypotheses. Standard and mixed variational formulations of the governing equations are then developed and the existence theories relating to these formulations are analysed.

2.1 Notation and Preliminary Definitions

In our analysis of the continuous problem we will make use of the following notation and definitions.

The inner product and associated norm on the space $L^2(0,1)$ of square integrable functions are respectively defined by

$$\langle u, v \rangle = \int_0^1 u(s)\, v(s)\, ds$$

and

$$\| u \| = \langle u, u \rangle^{\frac{1}{2}} \qquad \text{for all } u, v \in L_2(0,1).$$

The Sobolev space $H^m(0,1)$ of functions which, together with their weak derivatives of order $\leq m$ are square integrable on $(0,1)$, is a Hilbert space with the inner product $\langle .,. \rangle_m$, where

$$\langle u, v \rangle_m = \sum_{k=0}^{m} \langle \frac{d^k u}{ds^k}, \frac{d^k v}{ds^k} \rangle \qquad \text{for all } u, v \in H^m(0,1).$$

The norm generated by this inner product is given by $\| u \|_m = \langle u, u \rangle_m^{\frac{1}{2}}$.

Extensive use will be made of the following inequalities (see [11], [9] or [6] for details). For an inner product space V, with inner product $\langle .,. \rangle$ and corrresponding norm $\| . \|$, we have for any u, v $\in V$:

the Schwarz inequality

$$| \langle u, v \rangle | \leq \langle u, u \rangle^{\frac{1}{2}} \langle v, v \rangle^{\frac{1}{2}}$$

and the triangle inequality

$$\|u+v\| \leq \|u\| + \|v\|.$$

We will also make good use of

Young's inequality

$$2ab \leq \eta\, a^2 + \frac{1}{\eta}\, b^2$$

for real numbers a, b and η where $\eta \neq 0$. Also note that if

$$\begin{aligned} a &\leq b+c \\ \text{then} \qquad a^2 &\leq 2(b^2+c^2). \end{aligned} \tag{2.1}$$

This follows by squaring the first equation and then applying Young's inequality, with $\eta = 1$, to middle term of the right hand side quadratic.

The continuous problem is posed in the subspace $H_0^1(0,1)$ of $H^1(0,1)$ defined by

$$H_0^1(0,1) = \{v \in H^1(0,1) : v(0) = v(1) = 0\}.$$

By the Poincaré-Friedrichs inequality one has

$$\|v\| \leq \|v'\| \qquad \text{for all } v \in H_0^1(0,1).$$

Thus the semi-norm defined by $|v|_1 = \|v'\|$ for all $v \in H^1(0,1)$ is a norm on $H_0^1(0,1)$ equivalent to the $H^1(0,1)$ norm. Henceforth, the space $H_0^1(0,1)$ will be associated with the semi-norm $|.|_1$.

The dual space $H^{-1}(0,1)$ of $H_0^1(0,1)$ is equipped with the norm

$$\|f\|_{-1} = \sup\left\{ \frac{|f(v)|}{|v|_1} \mid v \in H_0^1(0,1),\ v \neq 0 \right\}.$$

Three degrees of freedom are required in order to describe the rotation and displacements of the system. Hence we define the product space $X = (H_0^1(0,1))^3$, equipped with the norm

$$|y|_1 = (|\psi|_1^2 + |v|_1^2 + |z|_1^2)^{\frac{1}{2}} \qquad \text{for all } y = (\psi, v, z) \in X.$$

The dual space $X' = (H^{-1}(0,1))^3$ of X is equipped with the norm

$$\|F\|_{-1} = (\|f_r\|_{-1}^2 + \|f_t\|_{-1}^2 + \|f_n\|_{-1}^2)^{\frac{1}{2}} \qquad \text{for all } F = (f_r, f_t, f_n) \in X'.$$

2.2 The Governing equations

Geometry

Consider a thin, circular arch of length L and uniform cross sectional area A, which is fixed at the end points as shown in Figure 1. Let $\bar{s}$ be the arc length measured from one end along the centre line of the arch. The radius of the arch centre-line is R.

The arch is subject to a distributed load $\bar{\mathbf{F}}(\bar{s})$ applied along its length causing it to deform. We allow for only one plane of motion, namely the x-y cartesian plane and introduce the position vector $\mathbf{r}$ of the centreline of the arch. Deformation is subject to the Timoshenko hypotheses hence allowing for both shear and membrane deformation. Define local section

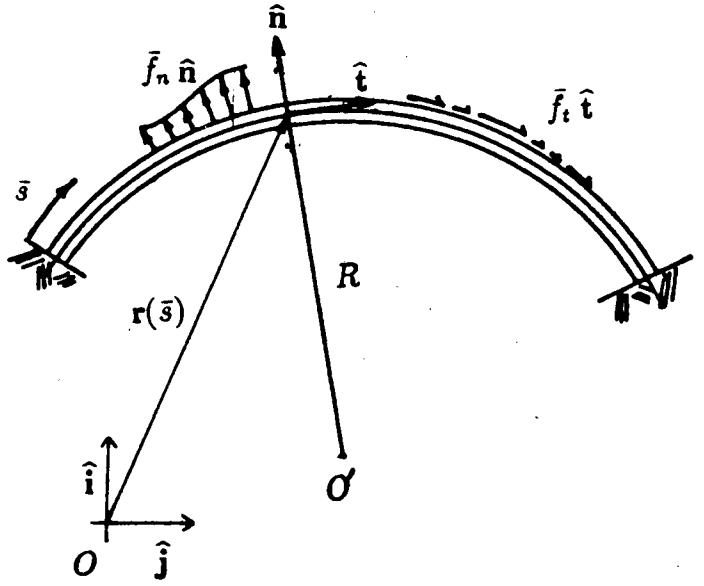

Figure 1: A uniform circular arch of radius R subject to an applied load $\bar{\mathbf{F}}$.

basis vectors; $\hat{\mathbf{b}}$ normal to the plane, and $\hat{\mathbf{n}}$ and $\hat{\mathbf{t}}$ which are respectively normal and tangential to the arch. For future analysis, we will require the following expressions involving the local basis vectors:

$$\hat{\mathbf{t}} = \frac{d\mathbf{r}}{d\bar{s}}, \tag{2.2}$$

$$\frac{d\hat{\mathbf{t}}}{d\bar{s}} = -\frac{\hat{\mathbf{n}}}{R} \quad \text{and} \quad \frac{d\hat{\mathbf{n}}}{d\bar{s}} = \frac{\hat{\mathbf{t}}}{R}. \tag{2.3}$$

The derivation of these expressions is given in Appendix A.

The behaviour of the arch is fully described by three sets of equations; the equilibrium, the kinematic and the constitutive equations and must satisfy certain boundary conditions. We now proceed to discuss each of these sets of equations.

The equations of equilibrium

The circular arch is subject to both external and internal forces. The *equations of equilibrium* describe the relation between these two forces when the arch is in equilibrium.

The *external* forces on a body are in the form of applied loads (including the weight of the body), or support reactions. In general, external forces are independent of the deformation and material properties of the body. We describe the external forces acting on the arch in the form of a distributed applied load $\bar{\mathbf{F}}$ per unit length which, in terms of the local section bases, may be written as

$$\bar{\mathbf{F}}(\bar{s}) = \bar{f}_t(\bar{s})\hat{\mathbf{t}} + \bar{f}_n(\bar{s})\hat{\mathbf{n}}\,, \qquad 0 \le \bar{s} \le L.$$

The internal forces are defined in terms of the stress resultants[1] which develop at any cross section of the arch. Consider a cross section of the arch, at some arbitrary point $\mathbf{P}$ a distance

[1]Stress resultant: the integral of a given stress distribution over the area of a cross sectional plane.

For this equation to be satisfied, the coefficients of the orthogonal vectors $\hat{\mathbf{t}}$ and $\hat{\mathbf{n}}$ must both be zero. Hence

$$\frac{dN}{d\bar{s}} + \frac{Q}{R} + \bar{f}_t = 0 \tag{2.4}$$

and

$$\frac{dQ}{d\bar{s}} - \frac{N}{R} + \bar{f}_n = 0. \tag{2.5}$$

Next, we take the vector sum of the moments about the origin to get

$$-M(0)\hat{\mathbf{b}} - \mathbf{r}(0) \times \{N(0)\hat{\mathbf{t}}(0) + Q(0)\hat{\mathbf{n}}(0)\} +$$

$$\int_0^{\bar{s}} \mathbf{r}(\xi) \times \{\bar{f}_t(\xi)\hat{\mathbf{t}}(\xi) + \bar{f}_n(\xi)\hat{\mathbf{n}}(\xi)\}\, d\xi + M(\bar{s})\hat{\mathbf{b}} + \mathbf{r}(\bar{s}) \times \{N(\bar{s})\hat{\mathbf{t}}(\bar{s}) + Q(\bar{s})\hat{\mathbf{n}}(\bar{s})\} = \mathbf{0}.$$

Differentiation of this equation with respect to $\bar{s}$ and the use of (2.3) leads to the equation

$$\mathbf{r}(\bar{s}) \times \{\bar{f}_t(\bar{s})\hat{\mathbf{t}}(\bar{s}) + \bar{f}_n(\bar{s})\hat{\mathbf{n}}(\bar{s})\} + \frac{dM}{d\bar{s}}\hat{\mathbf{b}} + \hat{\mathbf{t}} \times (N\hat{\mathbf{t}} + Q\hat{\mathbf{n}})$$

$$+\mathbf{r} \times (\frac{dN}{d\bar{s}}\hat{\mathbf{t}} - \frac{N}{R}\hat{\mathbf{n}} + \frac{dQ}{ds}\hat{\mathbf{n}} + \frac{Q}{R}\hat{\mathbf{t}}) = \mathbf{0}.$$

Since $\hat{\mathbf{t}} \times \hat{\mathbf{t}} = \mathbf{0}$ and $\hat{\mathbf{t}} \times \hat{\mathbf{n}} = \hat{\mathbf{b}}$, this equation becomes

$$\mathbf{r} \times (\frac{dN}{d\bar{s}} + \frac{Q}{R} + \bar{f}_t)\hat{\mathbf{t}} + \mathbf{r} \times (\frac{dQ}{d\bar{s}} - \frac{N}{R} + \bar{f}_n)\hat{\mathbf{n}} + (\frac{dM}{d\bar{s}} + Q)\hat{\mathbf{b}} = \mathbf{0}.$$

From (2.4), the coefficients of $\hat{\mathbf{t}}$ and $\hat{\mathbf{n}}$ are zero and hence this equation is equivalent to the condition

$$\frac{dM}{d\bar{s}} + Q = 0. \tag{2.6}$$

Equations (2.4), (2.5) and (2.6) are the *equations of equilibrium* of the system.

The kinematic equations

We now study the displacements and the deformation caused by the forces acting on the arch.

Since we have in-plane motion, the displacement component perpendicular to the x-y plane, and the rotation component about axes lying in the x-y plane are zero. We denote the displacement of the centre-line by $\bar{\mathbf{u}}(\bar{s})$, and express it in terms of the local basis in the form (see Figure 3)

$$\bar{\mathbf{u}} = \bar{u}\,\hat{\mathbf{t}} + \bar{w}\,\hat{\mathbf{n}}\ ,$$

so that $\bar{u}$ and $\bar{w}$ are respectively the tangential and normal displacement. The rotation of the centreline is given by

$$\bar{\boldsymbol{\phi}}\ (\bar{s}) = \bar{\phi}(\bar{s})\,\hat{\mathbf{b}}\ .$$

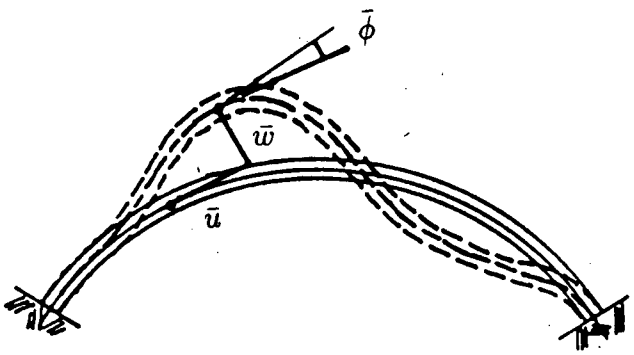

Figure 3: Tangential ($\bar{u}$) and normal ($\bar{w}$) displacement components, and rotation ($\bar{\phi}$) of centreline due to deformation of the arch.

At this point we introduce *generalised strains* as quantities which measure the deformation of the bar. Under rigid body motion, the bar displaces without deforming. So a suitable way of defining generalised strains is by identifying a set of quantities which vanish in a rigid body motion. Hence we proceed by deriving an expression for rigid body motion, and then find what functions of the displacement and rotation functions are zero in such a motion. Suppose that components $\bar{u}(0)$, $\bar{w}(0)$ and $\bar{\phi}(0)$ are imposed at the one end of the arch where

$\bar{s} = 0$. Then in a rigid body displacement, the rotation at a general point P is

$$\bar{\phi}(\bar{s}) = \bar{\phi}(0), \tag{2.7}$$

while the displacement written in vector terms will be given by

$$\bar{\mathbf{u}}(\bar{s}) = \bar{\mathbf{u}}(0) + \bar{\phi}(0)\,\hat{\mathbf{b}} \times [\mathbf{r}(\bar{s}) - \mathbf{r}(0)]. \tag{2.8}$$

Differentiation of equation (2.7) shows that

$$\frac{d\bar{\phi}}{d\bar{s}} = 0 \tag{2.9}$$

is a necessary condition for rigid body rotation. Also, from equation (2.8), a necessary condition for rigid body displacement is that

$$\begin{aligned} \frac{d\bar{\mathbf{u}}}{d\bar{s}} = \bar{\phi}(0)\,\hat{\mathbf{b}} \times \frac{d\mathbf{r}}{d\bar{s}} &= \bar{\phi}(\bar{s})\,\hat{\mathbf{b}} \times \hat{\mathbf{t}} \qquad \text{(from (2.2) and (2.7))}, \\ &= \bar{\phi}(\bar{s})\,\hat{\mathbf{n}}\,. \end{aligned}$$

Hence we can adopt as measures of deformation

$$\text{the vector quantity} \qquad \frac{d\bar{\mathbf{u}}}{d\bar{s}} - \bar{\phi}(\bar{s})\,\hat{\mathbf{n}} \tag{2.10}$$

$$\text{and the scalar quantity} \qquad \frac{d\bar{\phi}}{d\bar{s}}. \tag{2.11}$$

The vector quantity (2.10) is resolved into its tangential and normal components to give

$$\begin{aligned} \frac{d\bar{\mathbf{u}}}{d\bar{s}} - \bar{\phi}(\bar{s})\,\hat{\mathbf{n}} &= \frac{d}{d\bar{s}}(\bar{u}\,\hat{\mathbf{t}} + \bar{w}\hat{\mathbf{n}}) - \bar{\phi}\,\hat{\mathbf{n}} \\ &= \underbrace{\left(\frac{d\bar{u}}{d\bar{s}} + \frac{\bar{w}}{R}\right)}_{\varepsilon}\hat{\mathbf{t}} + \underbrace{\left(\frac{d\bar{w}}{d\bar{s}} - \frac{\bar{u}}{R} - \bar{\phi}\right)}_{\gamma}\hat{\mathbf{n}}\,. \end{aligned}$$

The quantity ε is known as the axial strain, and γ is known as the shear strain. We also denote by κ the bending strain $\frac{d\bar{\phi}}{d\bar{s}}$.

Suitable measures of deformation are therefore

$$\varepsilon = \frac{d\bar{u}}{d\bar{s}} + \frac{\bar{w}}{R}, \tag{2.12}$$

$$\gamma = \frac{d\bar{w}}{d\bar{s}} - \frac{\bar{u}}{R} - \bar{\phi}, \tag{2.13}$$

$$\kappa = \frac{d\bar{\phi}}{d\bar{s}}. \tag{2.14}$$

Equations (2.12), (2.13) and (2.14) are the kinematic equations of the system.

These kinematic equations can also be obtained by applying the Timoshenko hypotheses to the strain-displacement equations for a 3 dimensional body. The Timoshenko hypotheses for this problem are

$$\bar{u}(\bar{s}, y) = y\bar{\phi}(\bar{s}) \qquad \text{and} \qquad \bar{v}(\bar{s}, y) = \bar{v}(\bar{s}),$$

where y is the displacement in the $\hat{\mathbf{j}}$ direction.

The Constitutive Equations

The constitutive equations for a linear elastic solid relate the stress tensor $\boldsymbol{\sigma}$ and the strain tensor $\boldsymbol{\varepsilon}$ via the expression $\boldsymbol{\sigma} = \mathbf{C}\,\boldsymbol{\varepsilon}$, known as the generalised Hooke's law. The elements of the elastic constant matrix $\mathbf{C}$ are determined experimentally, according to the material behaviour of the structure. For a linear elastic circular arch, with one plane of motion, Hooke's law reduces to the following constitutive equations:

$$\begin{aligned} N &= AE\varepsilon, \\ Q &= kAG\gamma, \\ \text{and} \quad M &= EI\kappa. \end{aligned} \tag{2.15}$$

A is the cross sectional area, E is Young's modulus, I the moment of inertia, G the shear modulus and k is the shear correction factor. Since the arch is assumed uniform, quantities E, I, A and k are all positive constants.

The boundary conditions

The ends of the arch are clamped so that we have the homogeneous boundary conditions

$$\begin{aligned} \bar{u}(0) &= 0, \quad & \bar{u}(L) &= 0, \\ \bar{w}(0) &= 0, \quad & \bar{w}(L) &= 0, \\ \bar{\phi}(0) &= 0, \quad & \bar{\phi}(L) &= 0. \end{aligned}$$

Non-dimensionalisation

The system of equations may be nondimensionalised by setting

$$s = \frac{\bar{s}}{L}\ , \quad \phi(s) = \bar{\phi}(\bar{s})\ , \quad u(s) = \frac{\bar{u}(\bar{s})}{L}\ , \quad \text{and} \quad w(s) = \frac{\bar{w}(\bar{s})}{L}.$$

We also define the nondimensional generalised internal forces

$$n = \frac{NL^2}{EI}\ , \quad q = \frac{QL^2}{EI}\ , \quad m = \frac{ML}{EI}\ ,$$

and the nondimensional external forces

$$(f_t, f_n) = (\bar{f}_t, \bar{f}_n)\,\frac{L^3}{EI}\ .$$

Then, multiplying the equilibrium equations (2.4) and (2.5) by $\frac{L^3}{EI}$, and (2.6) by $\frac{L^2}{EI}$, we obtain the equilibrium equations in the nondimensional form

$$\begin{aligned} -n' - \beta q &= f_t, \\ -q' + \beta n &= f_n, \\ \text{and} \qquad -m' - q &= 0, \end{aligned} \tag{2.16}$$

where $\beta = \frac{L}{R}$. Note that the superscript prime denotes differentiation with respect to s.

From (2.12), (2.13) and (2.14), one has the nondimensional kinematic equations

$$\begin{aligned} \varepsilon(x) &= u' + \beta\, w, \\ \gamma(x) &= w' - \beta\, u - \phi, \\ \text{and} \qquad \kappa(x) &= \frac{1}{L}\phi'. \end{aligned} \tag{2.17}$$

Finally, from (2.15), one has the dimensionless constitutive equations

$$\begin{aligned} n &= d^{-1}\varepsilon, \\ q &= \nu d^{-1}\gamma, \\ \text{and} \quad m &= L\kappa, \end{aligned} \tag{2.18}$$

where $\nu = \frac{kG}{E}$ and $d = \frac{I}{AL^2}$.

By nondimensionalising, the thickness of the arch has been incorporated in the parameter d. Thus we are in a position to examine the dependence of a solution to the problem in relation to the thickness of the arch. Note too that, for thin arches, parameter d is much smaller than unity . Hence we limit the value of d to the interval $(0, 1]$, though many of the results will be valid in the limit as $d \to 0$.

2.3 Variational Formulation of the Standard Problem

We proceed to formulate the problem in weak or variational form. This will form the basis of the analysis, not least because it is the formulation on which finite element approximations are based.

Formulation of the Problem

The variational formulation is obtained as follows. We multiply the equations (2.16_1), (2.16_2) and (2.16_3) by arbitrary functions v, z and ψ respectively, in $H_0^1(0,1)$. Next we integrate these equations over the interval $[0,1]$ and use integration by parts and the boundary conditions to obtain

$$\begin{aligned} \int_0^1 (-nv' + \beta qv)\, ds + \int_0^1 f_t v\, ds &= 0, \\ \int_0^1 (-qz' - \beta nz)\, ds + \int_0^1 f_n z\, ds &= 0, \end{aligned}$$

$$\int_0^1 (-m\psi' + q\psi)\, ds \;=\; 0.$$

Applying the constitutive equations (2.18) gives

$$\begin{aligned} d^{-1}\int_0^1 (\,\varepsilon(x)v' - \nu\beta\,\gamma(x)v\,)ds &= \int_0^1 f_t v\, ds, \\ d^{-1}\int_0^1 (\,\nu\,\gamma(x)z' + \beta\,\varepsilon(x)z\,)ds &= \int_0^1 f_n z\, ds, \\ \int_0^1 (L\,\kappa\psi' - \nu\, d^{-1}\gamma(x)\psi\,)ds &= 0. \end{aligned}$$

Adding these three equations together and applying the kinematic equations (2.17) gives the variational problem

$$\int_0^1 \phi'\psi'\, ds + \nu d^{-1}\int_0^1 \gamma(x)\gamma(y)\, ds + d^{-1}\int_0^1 \varepsilon(x)\varepsilon(y)\, ds \;=\; \int_0^1 f_t v + f_n z\, ds. \quad (2.19)$$

Thus we have

The Standard Problem **S**: For any given applied load $F = (0, f_t, f_n) \in X'$ and $d \in (0, 1]$, find $x = (\phi, u, w) \in X$ such that

$$B_d(x, y) \;=\; F(y) \qquad \forall\, y = (\psi, v, z) \in X, \quad (2.20)$$

where $B_d : X \times X \mapsto I\!R$ is the symmetric bilinear form

$$\begin{aligned} B_d(x,y) &= \langle\, \phi', \psi' \,\rangle + \nu\, d^{-1}\,\langle\, \gamma(x), \gamma(y) \,\rangle + d^{-1}\,\langle\, \varepsilon(x), \varepsilon(y) \,\rangle \quad (2.21) \\ &= \langle\, \phi', \psi' \,\rangle + \nu\, d^{-1}\,\langle\, w' - \beta\, u - \phi, z' - \beta\, v - \psi \,\rangle + d^{-1}\,\langle\, u' + \beta\, w, v' + \beta\, z \,\rangle, \end{aligned}$$

and F is the linear functional on X defined by

$$F(y) \;=\; \langle\, f_t, v \,\rangle \;+\; \langle\, f_n, z \,\rangle. \quad (2.22)$$

Existence and Uniqueness

From the Lax-Milgram theorem [11], we recall that sufficient conditions for the existence of a unique solution to the problem **S** are that

(s_1) $B_d(.,.)$ is X-elliptic, ie. there exists a constant $\alpha > 0$ such that

$$B_d(y,y) \geq \alpha |y|_1^2 \qquad \forall y \in X;$$

(s_2) $B_d(.,.)$ is continuous, ie. there exists a constant $C > 0$ such that

$$|B_d(x,y)| \leq C|x|_1|y|_1 \qquad \forall x,y \in X;$$

(s_3) F is continuous, ie. there exists a constant $c > 0$ such that

$$|F(y)| \leq c|y|_1 \qquad \forall y \in X.$$

The X-ellipticity condition is immediate for the Timoshenko beam problem [13] via the Riesz representation theorem. For the standard formulation of the shallow arch problem [41] the proof of X-ellipticity involves a few manipulations using the triangle and Poincaré-Friedrich inequalities. These manipulations (or similar), however, do not work for the circular arch problem due mainly to the extra rotational variable in the shear term. Instead, a similar proof to that used by Ciarlet [6] in his analysis of the circular arch subject to the Kirchoff-Love hypotheses, is required (see also the proof of Korn's inequality in [7]). This proof of X-ellipticity is very lengthy, so we present the following lemmas before formulating the main existence theory for the standard problem.

Lemma 2.1 *There exist constants $\lambda > 0$ and μ such that*

$$B_d(y,y) \geq \lambda |y|_1^2 + \mu \|y\|^2.$$

Proof: In this proof repeated use is made of the Schwarz and Young's inequalities.

From (2.17),

$$\begin{aligned}
\|\varepsilon(y)\|^2 &= \|v'\|^2 + 2\beta\langle v', z'\rangle + \beta^2\|z\|^2 \\
&\geq \|v'\|^2 - 2\beta\|v'\|\|z\| && \text{(Schwarz inequality)} \\
&\geq \|v'\|^2 - \beta\left(\frac{1}{a}\|z\|^2 + a\|v'\|^2\right) && \text{(Young's inequality)} \\
&= (1-\beta a)\|v'\|^2 - \frac{\beta}{a}\|z\|^2
\end{aligned}$$

for some arbitrary, positive constant a. Choosing $\beta a \in (0,1)$, we have $1-\beta a = \lambda_1 > 0$. Thus

$$\|\varepsilon(y)\|^2 \geq \lambda_1 \|v'\|^2 + \mu_1 \|z\|^2 \qquad \text{(i)}$$

where constant $\mu_1 = -\frac{\beta}{a}$.

Similarly,

$$\begin{aligned} \|\gamma(y)\|^2 &= \|z'\|^2 - 2\langle z', \psi + \beta v\rangle + \|\psi + \beta v\|^2 \\ &\geq \|z'\|^2 - 2\|z'\|\,\|\psi + \beta v\| \\ &\geq (1-b)\|z'\|^2 - \frac{1}{b}\|\psi + \beta v\|^2, \qquad \text{(ii)} \end{aligned}$$

for some arbitrary, positive constant b. Now, using Young's inequality again we have

$$\begin{aligned} \|\psi + \beta v\|^2 &\leq \|\psi\|^2 + 2\beta\|\psi\|\,\|v\| + \beta^2\|v\|^2 \\ &\leq \|\psi\|^2 + \beta(c\|\psi\|^2 + \frac{1}{c}\|v\|^2) + \beta^2\|v\|^2 \\ &= (1+\beta c)\|\psi\|^2 + (\beta^2 + \frac{\beta}{c})\|v\|^2 \end{aligned}$$

where constant c is positive. Hence, substitution of this expression into (ii) gives

$$\|\gamma(y)\|^2 \geq (1-b)\|z'\|^2 - \frac{1}{b}(1+\beta c)\|\psi\|^2 - \frac{\beta}{b}(\beta + \frac{1}{c})\|v\|^2.$$

Choosing $b \in (0,1)$, gives $1-b = \lambda_2 > 0$ and

$$\|\gamma(y)\|^2 \geq \lambda_2\|z'\|^2 + \mu_2(\|\psi\|^2 + \|v\|^2) \qquad \text{(iii)}$$

where

$$\mu_2 = -\max\{\frac{1}{b}(1+\beta c), \frac{\beta}{b}(\beta + \frac{1}{c})\}.$$

Thus from (i) and (iii) we have

$$\begin{aligned} B_d(y,y) &= \|\psi'\|^2 + \nu d^{-1}\|z' - \beta v - \psi\|^2 + d^{-1}\|v' + \beta z\|^2 \\ &\geq \lambda(\|\psi'\|^2 + \|v'\|^2 + \|z'\|^2) + \mu(\|\psi\|^2 + \|v\|^2 + \|z\|^2) \end{aligned}$$

where

$$\lambda = \min\{\, 1,\ d^{-1}\lambda_1,\ \nu d^{-1}\lambda_2 \,\} \quad \text{and} \quad \mu = \min\{\, d^{-1}\mu_1,\ \nu d^{-1}\mu_2 \,\}.$$

Hence

$$B_d(y,y) \geq \lambda |y|_1^{\,2} + \mu \|y\|^2$$

where $\lambda > 0$. ∎

Lemma 2.2 *The mapping* $g : y \mapsto \sqrt{B_d(y,y)}$ *is a norm on* X.

Proof: The bilinear form $B_d(y,y)$ is clearly symmetric, non-negative and obeys the triangle inequality. So, in order to prove that $\sqrt{B_d(y,y)}$ defines a norm on X, we only need to show that $B_d(y,y)$ is positive definite. We do so by showing that $B_d(y,y) = 0$ corresponds to rigid body motion. Hence application of the boundary conditions will give $y = 0$.

Recall that in the derivation of the equilibrium equations we found that rigid body motion was defined by the two equations (2.7) and (2.8). That is, if the end of an arch undergoes the displacement $x(0) = (\,\psi(0), v(0), z(0)\,)$, the rotation at a general point on the bar is given by

$$\psi(s) = \psi(0), \qquad \text{(i)}$$

while the displacement is given by

$$\mathbf{v}(s) = \mathbf{v}(0) + \psi(0)\,\widehat{\mathbf{b}} \times (\mathbf{r}(s) - \mathbf{r}(0)) \qquad \text{(ii)}$$

where $\mathbf{v}(s) = v(s)\,\widehat{\mathbf{t}} + z(s)\,\widehat{\mathbf{n}}$, $\mathbf{r}$ is the position vector of the centreline of the arch and $\widehat{\mathbf{t}}$, $\widehat{\mathbf{n}}$ and $\widehat{\mathbf{b}}$ are the local bases vectors.

Recall also equations (2.3) which in non-dimensional form are expressed as

$$\frac{d\widehat{\mathbf{t}}}{ds} = -\beta\,\widehat{\mathbf{n}} \qquad \text{and} \qquad \frac{d\widehat{\mathbf{n}}}{ds} = \beta\widehat{\mathbf{t}}\,. \qquad \text{(iii)}$$

We now show that by setting $B_d(y,y) = 0$ we will obtain equations (i) and (ii) implying rigid body motion.

For any $y = (\psi, v, z) \in X$

$$B_d(y,y) = 0 \Rightarrow \begin{cases} \psi' = 0 & \text{(iv)} \\ z' - \beta v - \psi = 0 & \text{(v)} \\ v' + \beta z = 0. & \text{(vi)} \end{cases}$$

Integrating (iv) with respect to s immediately gives equation (i).

Equations (v) and (vi) are equivalent to the vector equation

$$(v' + \beta z)\,\hat{\mathbf{t}} + (z' - \beta v - \psi)\,\hat{\mathbf{n}} = \mathbf{0}. \qquad \text{(vii)}$$

Substitution of equations (iii) into equation (vii) therefore gives

$$\frac{d}{ds}(v\,\hat{\mathbf{t}} + z\,\hat{\mathbf{n}}) - \psi\,\hat{\mathbf{n}} = \mathbf{0}.$$

That is,

$$\begin{aligned} \frac{d\mathbf{v}}{ds} = \psi(s)\,\hat{\mathbf{n}} &= \psi(s)(\hat{\mathbf{b}} \times \hat{\mathbf{t}}) \\ &= \psi(0)\,\hat{\mathbf{b}} \times \frac{d\mathbf{r}}{ds} \qquad \text{(from (i) and 2.2).} \end{aligned}$$

Hence

$$\begin{aligned} \mathbf{v}(s) - \mathbf{v}(0) &= \int_0^s \frac{d\mathbf{v}(t)}{dt}\,dt \\ &= \psi(0)\,\hat{\mathbf{b}} \times \int_0^s \frac{d\mathbf{r}(t)}{dt}\,dt \\ &= \psi(0)\,\hat{\mathbf{b}} \times (\mathbf{r}(s) - \mathbf{r}(0)). \end{aligned}$$

So equation (ii) is satisfied, thus implying rigid body motion. Therefore, imposition of the boundary conditions $\psi(0) = 0$, $\mathbf{v}(0) = \mathbf{0}$ in equations (i) and (ii) implies $y = 0$, as required. ∎

We are now in a position to establish the existence theorem for the standard problem.

Theorem 2.1 **a.** *For any given $F \in X'$ and $d \in (0,1]$, there exists a unique solution $x = (\phi, u, w) \in X$ to problem (S).*

b. *There exists a constant C, independent of d, such that*

$$|x|_1 + d^{-1}\nu \|\gamma(x)\| + d^{-1} \|\varepsilon(x)\| \quad \leq \quad C \|F\|_{-1}. \tag{2.23}$$

Proof of a: Recall that we need to prove that $B_d(.,.)$ is X-elliptic and continuous, and that F is continuous.

We first show, by contradiction, that $B_d(.,.)$ is X-elliptic.

Assume $B_d(y,y)$ is not X-elliptic. Then there exists a sequence $\{y^k\} = \{(\psi^k, v^k, z^k)\} \in X$ such that

$$\lim_{k\to\infty} B_d(y^k, y^k) = 0 \quad \text{and} \quad |y^k|_1 = 1 \quad .$$

The sequence $\{y^k\}$ is bounded in X. Hence there exists a subsequence, denoted here also by $\{y^k\}$, such that $y^k \rightharpoonup y$ in X, where $y = (\psi, v, z)$ is in X. Also, since X is compactly embedded in $Y = L^2(0,1)^3$, we have $y^k \to y$ in Y.

Now, the functional $g{:}y \to B_d(y,y)$ is convex and continuous in X. Thus g is weakly lower semi-continuous, so that

$$\lim_{k\to\infty} \inf g(y^k) \geq g(y) \qquad \forall y \in X,$$

from which it follows that

$$B_d(y,y) \leq \lim_{k\to\infty} \inf B_d(y^k, y^k) = \lim_{k\to\infty} B_d(y^k, y^k) = 0,$$

the last step following from the assumption.

Hence $\quad B_d(y,y) = 0 \quad \Rightarrow \quad y = 0$ from lemma 2.2.

Now from lemma 2.1,

$$\begin{aligned} 0 = \lim_{k\to\infty} B_d(y^k, y^k) &\geq \lambda \lim_{k\to\infty} |y^k|_1^2 + \mu \lim_{k\to\infty} (\|\psi^k\|^2 + \|v^k\|^2 + \|z^k\|^2) \\ &= \lambda + \mu(\|\psi\|^2 + \|v\|^2 + \|z\|^2) \\ &= \lambda + \mu\|y\|^2 \\ &= \lambda \qquad \text{since} \quad y = 0. \end{aligned}$$

This is a contradiction since $\lambda > 0$. Thus $B_d(y, y)$ is X-elliptic.

Continuity of the bilinear form follows easily from application of the triangle and Poincaré inequalities. That is, given any $y = (\psi, v, z) \in X$ we have

$$\begin{aligned} \|\gamma(y)\| &\leq \|z'\| + \beta\|v\| + \|\psi\| \qquad \text{(triangle ineq.)} \\ &\leq \|z'\| + \beta\|v'\| + \|\psi'\| \qquad \text{(Poincaré ineq.)} \\ &\leq (2+\beta)|y|_1. \end{aligned}$$

Similarly

$$\|\varepsilon(y)\| \leq (1+\beta)|y|_1.$$

Hence for any $x, y \in X$ we have, using Schwarz' inequality,

$$\begin{aligned} |B_d(x,y)| &\leq \|\phi'\|\|\psi'\| + \eta d^{-1}\|\gamma(x)\|\|\gamma(y)\| + d^{-1}\|\varepsilon(x)\|\|\varepsilon(y)\| \\ &\leq (1 + \nu d^{-1}(2+\beta)^2 + d^{-1}(1+\beta)^2)|x|_1|y|_1, \end{aligned}$$

and therefore $B_d(.,.)$ is continuous.

Clearly F is continuous since

$$\begin{aligned} |< F, y >| &\leq |(f_t, w) + (f_n, z)| \\ &\leq \|f_t\|\|w\| + \|f_n\|\|z\| \\ &\leq C|y|_1 \quad \text{where } C = \max\{\|f_t\|, \|f_n\|\}. \end{aligned}$$

Hence, by the Lax-Milgram theorem there exists a unique solution to problem S.

Proof of b: Suppose that for any $\rho \in L^2(0,1)$ functions $y_1, y_2 \in X$ could be constructed such that

$$\varepsilon(y_1) = \rho, \qquad \gamma(y_1) = 0, \qquad |y_1|_1 \leq c_1 \|\rho\| \qquad \text{(i)}$$

and

$$\varepsilon(y_2) = 0, \qquad \gamma(y_2) = \rho, \qquad |y_2|_1 \leq c_2 \|\rho\|, \qquad \text{(ii)}$$

where c_1 and c_2 are positive constants.

Then by setting $\rho = \varepsilon(x)$, $y_1 = (\psi, v, z)$, we get from (i) that

$$\begin{aligned} \langle \phi', \psi' \rangle + d^{-1} \|\varepsilon(x)\|^2 &= F(y_1) \\ \Rightarrow \quad d^{-1} \|\varepsilon(x)\|^2 &\leq \|F\|_{-1} |y_1|_1 + \|\phi'\| \|\psi'\| \quad \text{(Schwarz ineq.)} \\ &\leq (\|F\|_{-1} + |x|_1)\, |y_1|_1. \qquad \text{(iii)} \end{aligned}$$

But, by X-ellipticity of $B_d(.,.)$ and (2.20), it follows that

$$|x|_1 \leq \frac{1}{\alpha} \|F\|_{-1}. \qquad \text{(iv)}$$

Applying this result and the inequality in (i) to (iii) gives

$$\begin{aligned} d^{-1} \|\varepsilon(x)\|^2 &\leq c_1 (\|F\|_{-1} + \frac{1}{\alpha} \|F\|_{-1}) \|\varepsilon(x)\| \\ \Rightarrow \quad d^{-1} \|\varepsilon(x)\| &\leq C_1 \|F\|_{-1} \qquad \text{(v)} \end{aligned}$$

where $C_1 = \max\{c_1, \frac{c_1}{\alpha}\}$ is positive.

Similarly, setting $\rho = \gamma(x)$ we get from (ii) that

$$\nu d^{-1} \|\gamma(x)\|^2 \leq (\|F\|_{-1} + |x|_1)\, |y_2|_1;$$

and applying (iv) and the inequality of (ii) gives

$$\nu d^{-1} \|\gamma(x)\| \leq C_2 \|F\|_{-1}, \qquad \text{(vi)}$$

where $C_2 = \max\{c_2, \frac{c_2}{\alpha}\}$.

Hence combining (iv), (v) and (vi) we get

$$|x|_1 + d^{-1}\nu\,\|\gamma(x)\| + d^{-1}\,\|\varepsilon(x)\| \quad \leq \quad C\,\|F\|_{-1}$$

where $C = \max\{C_1, C_2\}$ is positive as required.

To construct a function $y_1 = (\psi, v, z) \in X$ satisfying (i), we set

$$z(s) = s(1-s)(a + bs + cs^2) \qquad \text{(vii)}$$

where a, b and c are constants yet to be determined. Now for any $\rho \in L^2(0,1)$, set

$$\varepsilon(y_1) \equiv v' + \beta\, z \;=\; \rho$$

and apply the boundary condition $v(0) = 0$ to obtain

$$v(s) \;=\; \int_0^s (\rho(t) - \beta\, z(t))\, dt. \qquad \text{(viii)}$$

Similarly we set

$$\gamma(y_1) \equiv z' - \beta\, v - \psi \;=\; 0$$

which, upon substitution of (viii) gives

$$\psi(s) \;=\; z'(s) - \beta \int_0^s (\rho(t) - \beta\, z(t)\, dt. \qquad \text{(ix)}$$

Now we impose the remaining boundary conditions, in order to determine the values of a,b and c. The boundary condition $v(1) = 0$ applied to (viii) gives

$$\beta \int_0^1 z(t)\, dt \;=\; \int_0^1 \rho(t)\, dt. \qquad \text{(x)}$$

Applying the boundary condition $\psi(0) = 0$ to (ix) gives $a = 0$, while $\psi(1) = 0$ implies that

$$z'(1) + \beta^2 \int_0^1 z(t))\, dt \;=\; \beta \int_0^1 \rho(t)\, dt$$

$$\text{or} \qquad z'(1) \;=\; 0, \qquad \text{(from (x))}$$

$$\text{from which we obtain} \qquad b \;=\; -c.$$

Substituting this result into (x) gives

$$b = \frac{30}{\beta} \int_0^1 \rho(t)\, dt.$$

Hence from (vii),

$$z(s) = \frac{30}{\beta}\left(\int_0^1 \rho(t)\, dt \right) s^2(1-s)^2 \qquad \text{(xi)}$$

and thus there exists some constant c_3 such that $|z|_1 \leq c_3 \|\rho\|$. Substitution of (xi) into equations (viii) and (ix) yields the relations $|v|_1 \leq c_4 \|\rho\|$ and $|\psi|_1 \leq c_5 \|\rho\|$ for appropriate constants c_4 and c_5. Thus

$$|y_1|_1 \leq c_1 \|\rho\|$$

as required.

In a similar way, a function $y_2 \in X$ can be constructed which satifies (ii). ■

Note

1. In theorem 2.1b) one shows that the solution x of (2.20) depends continuously on the data in the sense of inequality (2.23).

2. From (2.23), as the parameter $d \to 0$, the shear and axial strain go to zero, that is

$$u' + \beta w = 0 \qquad \text{and} \qquad w' - \beta u - \phi = 0, \qquad (2.24)$$

and the Kirchhoff-Love-Poisson hypothesis is recovered. Hence the Timoshenko-Reissner-Mindlin hypothesis can be seen as a penalty method for the Kirchhoff-Love-Poisson hypothesis.

The first of equations (2.24) is known as the inextensional strain condition while the second is the classical Kirchhoff condition that precludes transverse shear strains.

2.4 A Mixed Formulation

In the mixed formulation the axial and shear forces are retained as variables in the form of Lagrange multipliers. Hence we now need to choose two subspaces corresponding to the forces and the displacements, that is, the Lagrange multiplier space and the primal space respectively. We now formulate an equivalent mixed variational formulation to problem **S** and, using Brezzi's theorem [18], we establish the existence of a unique solution for any value of the thickness parameter d.

Formulation of the Problem

For any given $d \in (0,1]$, introduce the Lagrange multiplier $p = (\xi, \eta) \in (L^2(0,1))^2 = Q$ and pose the

Mixed Variational Problem **M**. Find $(x,p) \in X \times Q$ such that

$$a(x,y) + b(y,p) = F(y) \tag{2.25}$$

$$-d\langle p,q \rangle + b(x,q) = 0 \tag{2.26}$$

for all $y \in X$ and $q = (\kappa, \lambda) \in Q$, where

$$a: X \times X \mapsto I\!R \quad , \quad a(x,y) = \langle \phi', \psi' \rangle,$$

$$b: X \times Q \mapsto I\!R \quad , \quad b(x,q) = \nu \langle \gamma(x), \kappa \rangle + \langle \varepsilon(x), \lambda \rangle.$$

The mixed problem **M** and the standard problem **S** are equivalent since, from (2.26) one has

$$\nu \langle \gamma(x), \kappa \rangle + \langle \varepsilon(x), \lambda \rangle - d\,[\langle \xi, \kappa \rangle + \langle \eta, \lambda \rangle] = 0 \quad \forall (\kappa, \lambda) \in Q$$

$$\Rightarrow \qquad \langle \nu\,\gamma(x) - d\xi\,,\, \kappa \rangle + \langle \varepsilon(x) - d\eta\,,\, \lambda \rangle = 0$$

for all (κ, λ) in Q. Hence taking $\lambda = 0$, we get

$$\xi = \nu d^{-1}\,\gamma(x); \tag{2.27}$$

while taking $\kappa = 0$ gives

$$\eta = d^{-1}\,\varepsilon(x). \tag{2.28}$$

Substituting these values of ξ and η into (2.25) yields the standard formulation. The above steps are reversible, hence we can conclude that the mixed and standard formulations are equivalent.

Note that, by definition of γ and ε we see from (2.27) and (2.28), the Lagrange multipliers ξ and η have a definite physical meaning; namely the non-dimensional shear and axial forces, respectively.

Existence and Uniqueness

Next we need to show that problem **M** has a unique solution. Brezzi [18] formulated conditions for the existence of a unique solution to mixed variational problems with $d = 0$. These were later modified by Arnold [13] to include the case $d \in (0, 1)$. The conditions are:

(m_1) a is symmetric and positive semidefinite;

(m_2) there exists a constant $C_1 > 0$ such that

$$a(y, y) \geq C_1 |y|_1^2$$

for all $y \in Y$, where

$$\begin{aligned} Y &= \{y \in X : b(y, q) = 0 \quad \forall q \in Q\} \\ &= \{y \in X : \gamma(y) = 0 \text{ and } \varepsilon(y) = 0\}. \end{aligned}$$

(m_3) there exists a constant $C_2 > 0$ such that, given any $q \in Q$, there exists nonzero $y \in X$ such that

$$b(y, q) \geq C_2 \|q\|_Q |y|_1.$$

Condition (m_1) is clearly satisfied. To prove (m_2) recall that, by X-ellipticity of $B_d(.,.)$, we have

$$B_d(y,y) \geq \alpha |y|_1^2$$

for all $y \in X$. But for any $y \in Y$,

$$B_d(y,y) = a(y,y)$$

and hence

$$a(y,y) \geq \alpha |y|_1^2 \qquad \text{for all } y \in Y.$$

Condition (m_3) is established by application of the proof of theorem 2.1(b). That is, we show that for any given $q = (\kappa, \lambda) \in Q$, it is possible to construct functions $y_1, y_2 \in H_0^1(0,1)$ such that

$$\varepsilon(y_1) = \lambda, \qquad \gamma(y_1) = 0, \qquad |y_1|_1 \leq c_1 \|\lambda\|; \qquad \text{(i)}$$

and

$$\varepsilon(y_2) = 0, \qquad \gamma(y_2) = \kappa, \qquad |y_2|_1 \leq c_2 \|\kappa\| \qquad \text{(ii)}$$

for some constants c_1 and c_2. Hence taking $y = y_1 + y_2$ and using (i) and (ii), we get

$$\begin{aligned} b(y,q) &= b(y_1,q) + b(y_2,q) \\ &= \|\lambda\|^2 + \nu\|\kappa\|^2 \\ &\geq c\|q\|^2 \qquad \text{(iii)} \end{aligned}$$

where $c = \min\{1, \nu\}$. Now since

$$\begin{aligned} |y|_1 &\leq |y_1|_1 + |y_2|_1 \qquad \text{(triangle ineq.)} \\ &\leq c_1\|\lambda\| + c_2\|\kappa\| \\ &\leq c'\|q\| \end{aligned}$$

where $c' = \max\{c_1, c_2\}$, we get, by applying this result to (iii) that

$$b(y,q) \geq C_2 \|q\| |y|_1$$

where $C_2 = \frac{c}{c'}$.

The construction of functions $y_1, y_2 \in X$ satisfying (i) is the same as that used in the proof of theorem 2.1 b and is therefore omitted. ■

3 Finite Element Approximations

We now construct finite element approximations of the standard and mixed variational formulations. From past experience (eg. [13] [26] [42]) we note that the approximation to the standard problem will exhibit shear and membrane locking. Hence we will be particularly interested in analysing the stability and convergence of the finite element approximation to the mixed problem.

3.1 The Galerkin Method of Approximation

Approximations to the standard and mixed formulations can be done via the Galerkin method. This method consists of posing the problems in finite dimensional subspaces of the continuous space. For example, in approximating the standard formulation **S** we define a linear subspace X^h of X, which is spanned by n basis functions N_i, $i = 1, 2, \ldots, n$. Hence we can approximate the solution x, to problem **S**, by

$$x_h = \sum_{i=1}^{n} x_i N_i$$

for constants $x_i \in I\!R$. This is the essence of the Galerkin method of approximation.

Note that the index h is a parameter between 0 and 1 related to the dimension of X^h, and whose magnitude gives some indication of how close X^h is to X. The mesh parameter h is related to the dimension of X^h such that, as $n \to \infty$, $h \to 0$. We would like to choose basis functions N_i of X^h such that $\bigcup_{0<h<1} X^h$ is dense in X. The finite element method provides a general and systematic technique for constructing such basis functions.

3.2 Notation and Preliminary Definitions

When applying the finite element method, the interval $[0, 1]$ is partitioned into E subintervals $\Omega_e \equiv [s_{e-1}, s_e]$ where $0 < s_0 < s_1 < \ldots < s_e < \ldots < s_E = 1$. The mesh parameter is defined

by $h = \max\{|s_e - s_{e-1}|: e = 1, \ldots, E\}$, and the mesh refinements are assumed to be quasi-uniform. That is, there exists a constant $\eta > 0$ such that

$$\frac{\min\limits_e | s_e - s_{e-1} |}{\max\limits_e | s_e - s_{e-1} |} \geq \eta.$$

Let P_r^h denote the space of functions whose restrictions to the subintervals Ω_e are polynomials of degree r, that is,

$$P_r^h = \{v \in L^2(0,1) : v|_{\Omega_e} \in P_r(\Omega_e),\ e = 1, \ldots, E\}.$$

We also define

$$P_{r,0}^h = P_r^h \cap C[0,1] \quad \text{and} \quad \bar{P}_{r,0}^h = P_{r,0}^h \cap H_0^1(0,1).$$

Note that $P_r^h \subset L^2(0,1)$ and that elements of P_r^h are generally discontinuous at inter-element boundaries (see figure 4).

As was the case in [35] and [42], the same order of polynomial degrees will be used for the approximations of ϕ, u and v, and hence we define the subspace X^h of X by

$$X^h = (\bar{P}_{r,0}^h)^3. \tag{3.1}$$

The use of different order polynomials for approximating the rotation and displacement terms would lead to a more complex approximating scheme without any real increase in overall accuracy and convergence.

The finite dimensional subspace Q^h of Q is chosen to be

$$Q^h = (P_{r-1}^h)^2, \tag{3.2}$$

while the L^2–orthogonal projection onto P_{r-1}^h is denoted by π_{r-1}. That is, given $v \in L^2(0,1)$,

$$\langle v - \pi_{r-1} v, v_h \rangle = 0 \quad \text{for all } v_h \in P_{r-1}^h.$$

The L^2–orthogonal projection onto $(P^h_{r-1})^3$, also denoted π_{r-1}, is defined as

$$\langle\, y - \pi_{r-1}y, y_h \,\rangle = 0 \quad \text{for all } y_h \in (P^h_{r-1})^3,\ y \in (L^2(0,1))^3.$$

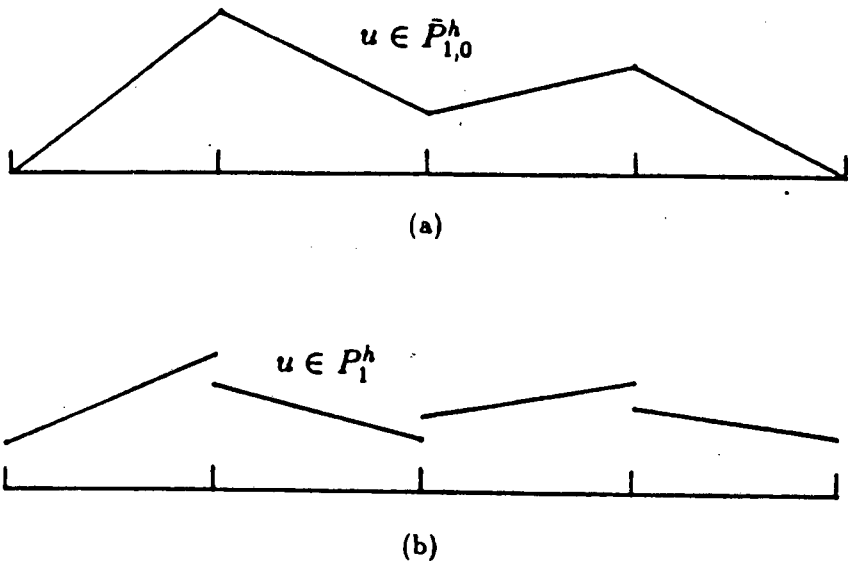

Figure 4: Examples of a function u belonging to (a) $\bar{P}^h_{r,0}$ and (b) P^h_r, for $r = 1$.

3.3 The Discrete Standard and Mixed Problems

We now formulate the discrete versions of the standard and mixed problems and establish the relationship between them. The existence of unique solutions to these problems is also confirmed.

Formulation of the Problem

The finite element formulation of the standard and mixed problems are, firstly, the

Discrete Standard Problem $\mathbf{S}_h$: find $x_h = (\phi_h, u_h, w_h) \in X^h$ such that

$$B_d(x_h, y_h) = F(y_h) \qquad \forall y_h = (\psi_h, v_h, z_h) \in X^h\,; \tag{3.3}$$

and, secondly, the

Discrete Mixed Problem $\mathbf{M}_h$: find $x_h = (\phi_h, u_h, w_h) \in X^h, p_h = (\xi_h, \eta_h) \in Q^h$ such that

$$a(x_h, y_h) + b_h(y_h, p_h) = F(y_h) \qquad \forall\, y_h \in X^h \tag{3.4}$$

$$-d\,\langle\, p_h, q_h \,\rangle + b_h(x_h, q_h) = 0 \qquad \forall\, q_h \in Q^h. \tag{3.5}$$

Unlike the continuous case, problems $\mathbf{S}_h$ and $\mathbf{M}_h$ are not equivalent. To see this, we note that equation (3.5) is equivalent to the equation

$$\nu\,\langle\, d^{-1}\,(w_h' - \beta\, u_h - \phi_h) - \xi_h\,,\, \kappa_h \,\rangle + \langle\, d^{-1}\,(u_h' + \beta\, w_h) - \eta_h\,,\, \lambda_h \,\rangle = 0.$$

Hence, from the projection theorem we get

$$\begin{pmatrix} \xi_h \\ \eta_h \end{pmatrix} = \pi_{r-1} \begin{pmatrix} \nu\, d^{-1}\, \gamma(x_h) \\ d^{-1}\, \varepsilon(x_h) \end{pmatrix}, \tag{3.6}$$

so that the discrete shear and axial forces can be expressed as L^2 projections of $\nu\, d^{-1}\, \gamma(x_h)$ and $d^{-1}\, \varepsilon(x_h)$ respectively, onto P^h_{r-1}. By substituting (3.6) into equation (3.4), we are able to eliminate the Lagrange multipliers to obtain

Problem $\mathbf{S}_{h\pi}$: find $x_h \in X_h$ such that

$$\mathcal{B}_d(x_h, y_h) = F(y_h) \quad \forall\, y_h \in X^h$$

where

$$\mathcal{B}_d(x_h, y_h) = a(x_h, y_h) + \nu\, d^{-1}\,\langle\, \pi_{r-1}\gamma(x_h), \pi_{r-1}\gamma(y_h) \,\rangle + d^{-1}\,\langle\, \pi_{r-1}\varepsilon(x_h), \pi_{r-1}\varepsilon(y_h) \,\rangle. \tag{3.7}$$

Therefore in the discrete case, the standard and mixed problems are no longer equivalent. Instead, problem $\mathbf{M}_h$ is equivalent to problem $\mathbf{S}_{h\pi}$.

Existence and Uniqueness

Existence of a unique solution to the discrete standard problem is easily proved since X^h is a subspace of X and hence, since $B_d(.,.)$ is X-elliptic, it is also X^h-elliptic. The proofs

of continuity conditions (s_2) and (s_3) remain valid in X^h and therefore we have a unique solution to problem $\mathbf{S}_h$.

The remainder of this section will deal with the existence of a unique solution to problem $\mathbf{M}_h$. In particular, we show that such approximate solutions to the mixed problem are stable and convergent.

Sufficient conditions for the existence of a unique solution to problem M_h are given by the following discrete versions of the conditions (m_1) - (m_3):

(m_{h1}) $a(.,.)$ is symmetric and positive semi-definite;

(m_{h2}) $a(.,.)$ is Y^h-elliptic; that is, there exists a constant $\alpha_h > 0$ such that

$$\begin{aligned} a(y_h, y_h) &\geq \alpha_h |y_h|_1^2 \quad \forall y_h \in Y^h, \\ \text{where} \quad Y^h &= \{y_h \in X^h : b(y_h, q_h) = 0 \quad \forall q_h \in Q^h\} \\ &= \{y_h \in X^h : \pi_{r-1}\gamma(y_h) = 0,\ \pi_{r-1}\varepsilon(y_h) = 0\}; \end{aligned}$$

(m_{h3}) $b(.,.)$ satisfies the discrete Brezzi condition; that is,

there exists a constant $C_h > 0$ such that, given any $q_h \in Q_h$, there exists a nonzero $y_h \in X^h$ such that

$$b(q_h, y_h) \geq C_h \| q_h \| |y_h|_1.$$

Note that, for the convergence result, we will also require that the constants α_h and C_h be independent of h. We proceed to show that all these conditions hold for problem $\mathbf{M}_h$.

Lemma 3.1 *The bilinear form $a(.,.)$ is Y^h-elliptic for sufficiently small h.*

Proof: In order to prove this condition we require the following interpolation error estimate from finite element interpolation theory (see [6], [11] for a proof) :

For any $u \in H^1(0,1)$, there exists a constant c, independent of h, such that

$$\| u - \pi_{r-1} u \| \leq ch | u |_1 .$$

Now since $u_h \in H^1(0,1)$, we may write

$$\| u_h - \pi_{r-1} u_h \| \leq ch | u_h |_1 .$$

Applying this result to the shear and membrane terms of the bilinear form of (3.7) we get that, for any $y_h \in X^h$,

$$\begin{aligned} \| \varepsilon(y_h) \| &= \| v_h' + \beta z_h \| \\ &= \| v_h' + \beta z_h + \beta \pi_{r-1} z_h - \beta \pi_{r-1} z_h \| \\ &\leq \| v_h' + \beta \pi_{r-1} z_h \| + \beta \| z_h - \pi_{r-1} z_h \| \\ &\leq \| \pi_{r-1} \varepsilon(y_h) \| + c\beta h | z_h |_1 . \qquad \text{(i)} \end{aligned}$$

Similarly,

$$\begin{aligned} \| \gamma(y_h) \| &= \| z_h' - \beta v_h - \psi_h \| \\ &\leq \| z_h' - \beta \pi_{r-1} v_h - \pi_{r-1} \psi_h \| + \beta \| \pi_{r-1} v_h - v_h \| + \| \pi_{r-1} \psi_h - \psi_h \| \\ &\leq \| \pi_{r-1} \gamma(y_h) \| + ch(\beta | v_h |_1 + | \psi_h |_1). \qquad \text{(ii)} \end{aligned}$$

Hence, using the X-ellipticity of B_d, with $d = 1$, and applying inequalities (i) and (ii), we get

$$\begin{aligned} \alpha | y_h |_1^{\,2} &\leq B_1(y_h, y_h) \\ &= \| \psi_h' \|^2 + \nu \| \gamma(y_h) \|^2 + \| \varepsilon(y_h) \|^2 \\ &\leq \| \psi_h' \|^2 + 2\nu \| \pi_{r-1} \gamma(y_h) \|^2 + 2 \| \pi_{r-1} \varepsilon(y_h) \|^2 + C | y_h |_1^{\,2} \qquad \text{(ineq. (2.1))} \\ &\leq 2\mathcal{B}_1(y_h, y_h) + C | y_h |_1^{\,2} \\ &\leq 2\mathcal{B}_d(y_h, y_h) + C | y_h |_1^{\,2} \end{aligned}$$

where $C = 2c^2h^2 \max\{1, \beta^2\}$. Therefore

$$\alpha_h |y_h|_1^2 \leq \mathcal{B}_d(y_h, y_h) \quad \forall y_h \in X^h,$$

where $\alpha_h = \frac{1}{2}(\alpha - Ch^2)$. Hence we can find an h_0 such that $\alpha - Ch_0^2 > \varepsilon$ for any small $\varepsilon > 0$. Therefore when $h \leq h_0$ there exists an $\alpha_h > 0$, independent of h, such that

$$\begin{aligned} \alpha_h |y_h|_1^2 &\leq \mathcal{B}_d(y_h, y_h) \\ &= a(y_h, y_h) \quad \text{for any} \quad y_h \in Y^h. \end{aligned}$$

■

Lemma 3.2 *There exists a constant $C_h > 0$, such that for any given $q_h \in Q_h$, there exist nonzero $y_h \in X^h$ such that*

$$b(q_h, y_h) \geq C_h \| q_h \| |y_h|_1.$$

Proof: To prove this, we adopt a similar approach to that used in verifying condition (m_3) in Theorem 2.1. That is, we show that for any $q_h = (\kappa_h, \lambda_h) \in Q^h$, we can construct functions y_{h1} and y_{h2} such that

$$\pi_{r-1}\varepsilon(y_{h1}) = \lambda_h\,, \qquad \pi_{r-1}\gamma(y_{h1}) = 0\,, \qquad |y_{h1}|_1 \leq C_1 \| q_h \|\,; \tag{i}$$

and

$$\pi_{r-1}\varepsilon(y_{h2}) = 0\,, \qquad \pi_{r-1}\gamma(y_{h2}) = \kappa_h\,, \qquad |y_{h2}|_1 \leq C_2 \| q_h \| \tag{ii}$$

where C_1 and C_2 are constants independent of h. Then, by taking $y_h = y_{h1} + y_{h2}$ we obtain condition (m_{h3}) since

$$\begin{aligned} b(y_h, q_h) &= \nu\langle \gamma(y_h), \kappa_h \rangle + \langle \varepsilon(y_h), \lambda_h \rangle \\ &= \nu\langle \pi_{r-1}\gamma(y_h), \kappa_h \rangle + \langle \pi_{r-1}\varepsilon(y_h), \lambda_h \rangle \\ &= \nu\langle \pi_{r-1}\gamma(y_{h1}) + \pi_{r-1}\gamma(y_{h2}), \kappa_h \rangle + \langle \pi_{r-1}\varepsilon(y_{h1}) + \pi_{r-1}\varepsilon(y_{h2}), \lambda_h \rangle \end{aligned}$$

$$= \nu \| \kappa_h \|^2 + \| \lambda_h \|^2$$

$$\geq \min\{1, \nu\} \| q_h \|^2$$

$$\geq C \| q_h \| \, | y_h |_1$$

where $C = \dfrac{\min\{1, \nu\}}{\max\{C_1 + C_2)\}}$.

In order to construct a function $y_{h1} = (\psi_h, v_h, z_h) \in X^h$ which satisfies (i), we choose for the case $r > 1$, two polynomials m and n of degree r over the interval $[0, 1]$, with the properties

$$m(0) = m(1) = n(0) = n(1) = 0;$$

also, if

$$M(s) = \int_0^s \pi_{r-1} m(t)\, dt \qquad \text{and} \qquad N(s) = \int_0^s \pi_{r-1} n(t)\, dt,$$

then m and n are chosen such that

$$M(1) \neq 0, \; N(1) \neq 0 \quad \text{and} \quad \delta \equiv \int_0^1 \pi_{r-1} M(s)\, ds - \frac{M(1)}{N(1)} \int_0^1 \pi_{r-1} N(s)\, ds \neq 0.$$

For the case $r = 1$ we choose two piecewise-linear functions m and n which satisfy the conditions given above. Note that there is no problem, in practice, to construct such polynomials or linear functions.

We now set $f_h(s) = am(s) + bn(s)$, where a and b are arbitrary constants yet to be determined. Solving the equation

$$z_h' = \pi_{r-1} f_h \qquad \text{(iii)}$$

subject to the boundary condition $z_h(0) = 0$, we obtain

$$z_h(s) = aM(s) + bN(s),$$

and applying the condition $z_h(1) = 0$ yields

$$aM(1) + bN(1) = 0. \qquad \text{(iv)}$$

Next, for given $\lambda_h \in P^h_{r-1}$ we solve

$$\pi_{r-1}\varepsilon(y_{h1}) \equiv v_h' + \beta\pi_{r-1}z_h = \lambda_h \quad \text{with} \quad v_h(0) = 0,$$

to obtain

$$v_h(s) = \int_0^s \lambda_h(t)\,dt - \beta\int_0^s \pi_{r-1}z_h(t)\,dt.$$

The condition $v_h(1) = 0$ gives

$$a\int_0^1 \pi_{r-1}M(s)\,ds + b\int_0^1 \pi_{r-1}N(s)\,ds = \beta^{-1}\int_0^1 \lambda_h(s)\,ds. \qquad \text{(v)}$$

Equations (iv) and (v) constitute a pair of equations in a and b which we solve to get

$$a = (\delta\beta)^{-1}\int_0^1 \lambda_h(s)ds \quad \text{and} \quad b = -\frac{M(1)}{N(1)}a.$$

Finally, we set

$$\psi_h(s) = f_h(s) - \beta v_h(s).$$

Clearly ψ_h is a member of $\bar{P}^h_{r,0}$ and by definition of (2.17) we have

$$\begin{aligned} \gamma(y_{h1}) &= \pi_{r-1}f_h(s) - f_h(s) \\ \Rightarrow \qquad \pi_{r-1}\gamma(y_{h1}) &= 0 \quad \text{since } \pi_{r-1} \text{ is idempotent.} \end{aligned}$$

Thus we have constructed functions $\psi_h, v_h, z_h \in \bar{P}^h_{r,0}$ which satisfy the first two conditions in (i). These functions also satisfy the third condition of (i) since

$$|a| \le c_1\|\kappa_h\| \quad \text{and} \quad |b| \le c_2\|\kappa_h\|$$

where $c_1 = (|\delta| \beta)^{-1}$ and $c_2 = c_1 \frac{M(1)}{N(1)}$. Letting $c = c_1 \| m' \| + c_2 \| n' \|$ we have $\| f_h' \| \leq c \| \kappa_h \|$. Therefore, from (iii) we have

$$\begin{aligned} \| z_h' \| &= \| \pi_{r-1} f_h \| \\ &\leq \| f_h \| \\ &\leq \| f_h' \| \qquad \text{(Poincaré ineq.)} \\ &\leq c \| \kappa_h \|. \end{aligned}$$

Similarly from (v) we have

$$\begin{aligned} \| v_h \| &\leq \| \kappa_h \| + \beta \| \pi_{r-1} z_h \| \\ &\leq \| \kappa_h \| + \beta \| z_h' \| \\ &\leq (1 + \beta c) \| \kappa_h \|, \end{aligned}$$

and from (vii)

$$\begin{aligned} \| \psi_h' \| &\leq \| f_h' \| + \beta \| v_h' \| \\ &\leq (c + \beta(1 + \beta c)) \| \kappa_h \|. \end{aligned}$$

Hence

$$y_{h1} \leq c_1 \| \kappa_h \| \leq c_1 \| q_h \|.$$

The construction of functions satisfying (ii) follows in a similar manner. ∎

We are now in a position to prove the existence of a unique solution to problem M_h.

Theorem 3.1 **a.** *Problem* M_h *has a unique solution.*

b. *If* $(x, p) \in X \times Q$ *is the solution of Problem M, then there is a constant* C*, independent of* h *and* d*, such that*

$$|x - x_h|_1 + \| p - p_h \| \leq C \inf\{ |x - y_h|_1 + \| p - q_h \| : \ y_h \in X_h, \ q_h \in Q^h \}. \qquad (3.8)$$

Proof of a: Condition (m_{h1}) is clearly satified and conditions (m_{h2}) and (m_{h3}) follow from lemma 3.1 and lemma 3.2 respectively.

Proof of b: The proof follows from theorem 3.1 of Brezzi [18]. ∎

Thus we have shown that although the standard and mixed formulations are equivalent their discrete counterparts $\mathbf{S}_h$ and $\mathbf{M}_h$ are not. This is as anticipated since finite element approximations to the mixed problem $\mathbf{M}_h$ are stable and convergent, while the discrete standard formulation $\mathbf{S}_h$ is expected to exhibit locking in the thin limit.

3.4 Selective Reduced Integration

In this section we formulate the reduced standard problem. We then examine the constraints that arise in the thin limit, from the shear and axial strains of the discrete standard problem $\mathbf{S}_h$, when piecewise linear approximation is used. We show that exact integration of these strain terms leads to additional spurious constraints which do not appear when reduced integration is applied. We then show why locking does not occur in the reduced standard formulation by showing its equivalence to the stable, convergent discrete mixed problem $\mathbf{M}_h$

Formulation of the Problem

In the finite element method, numerical integration is done via *Gaussian quadrature.* That is, given a function f that is integrable over the interval $[b, c]$, and using r-point Gaussian integration we have

$$\int_b^c f(x)\,dx \simeq \tfrac{1}{2}(c-b)\sum_{i=1}^{r} w_i \cdot f(p_i) \tag{3.9}$$

$$\equiv I_r[f], \tag{3.10}$$

where $p_i = \frac{1}{2}(c-b)\,a_i + \frac{1}{2}(c+b)$ and w_i and a_i represent the tabulated values of the weight functions and abscissae associated with the r gauss points respectively. Further we recall that a polynomial of degree $(2r-1)$ is integrated exactly by a gauss rule of order r.

Hence, if the interval $[0,1]$ has been partitioned into E subintervals $\Omega_e = [s_{e-1}, s_e]$, $e = 1, \ldots, E$, then, using r-point Gaussian quadrature, we can define the approximate L^2 inner product $\langle .,. \rangle_r$ by

$$\langle f_h, g_h \rangle_r = \sum_{e=1}^{E} (s_e - s_{e-1}) \sum_{i=1}^{r} w_i \cdot (f_h\, g_h)(\tfrac{1}{2}(s_e - s_{e-1})\, a_i + \tfrac{1}{2}(s_e + s_{e-1})), \qquad (3.11)$$

for any $f_h, g_h \in P_r^h$. Since the product of polynomials f_h and g_h is of the order $2r$, the above approximation would be exact for $r+1$ gauss points.

Applying reduced integration to the discrete standard problem $\mathbf{S}_h$ we can formulate the

Reduced Standard Problem **R**. For given $F \in X'$ and $d \in (0,1]$, find $\tilde{x}_h = (\tilde{\phi}_h, \tilde{u}_h, \tilde{v}_h) \in X^h$ such that

$$\langle \tilde{\phi}_h', \psi_h' \rangle + \nu d^{-1} \langle \gamma(\tilde{x}_h), \gamma(y_h) \rangle_r + d^{-1} \langle \varepsilon(\tilde{x}_h), \varepsilon(y_h) \rangle_r = F(y_h) \qquad (3.12)$$

for all $y_h \in X^h$.

Locking due to spurious constraints

Recall we noted from inequality (2.23) of the continuous standard problem that, as the thickness of the arch decreases, the states of inextensional and shearless deformations are enforced by the penalising of the shear and axial strains (referred to by some authors as the penalty strains [45] [4]) by the thickness parameter d. The enforcement of these deformation states at the element level implies that each polynomial coefficient of the penalty strains vanishes in the limit as the element thinness tends to zero. The resulting constraint equations are either properly coupled or spuriously uncoupled, resulting in the locking phenomenon

[39]. In reduced integration, only properly coupled penalty strains are produced and hence good convergence for thin one-dimensional structures is achieved.

We wish to analyse the constraints that arise from the shear and axial term of the discrete standard problem, in an attempt to illustrate the locking phenomenon. We do so by using the same approach as that of Prathap and Bhashyam [39] and Prathap [40], that is, by identifying the true and spurious constraints that arise when these terms are integrated exactly.

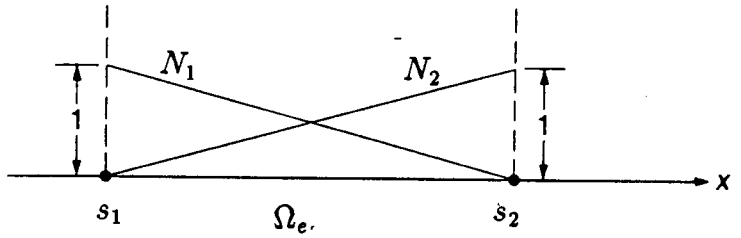

Figure 5: Linear local basis functions N_1 and N_2 over the element Ω_e.

We consider the case in which piecewise linear approximation is used. Then $N_1(s) = \frac{s_2 - s}{h}$ and $N_2(s) = \frac{s - s_1}{h}$ are local basis functions over the element Ω_e, where s_1 and s_2 are the nodal points and $h = s_2 - s_1$, as illustrated in figure 5. Hence, for any $u_h^{(e)} \in P_1(\Omega_e)$ we have $u_h^{(e)} = \sum_{i=1}^{2} u_i N_i$. For exact integration of the shear term $\| \gamma(x_h^{(e)}) \|^2$ and axial term $\| \varepsilon(x_h^{(e)}) \|^2$ we require 2-point Gaussian quadrature, for which the weights and abscissae are $w_1 = w_2 = 1$ and $a_1 = a_2 = \frac{-1}{\sqrt{3}}$ respectively. Hence, using p_1 and p_2 as defined in equation (3.9) it follows that

$$N_1(p_1) = N_2(p_2) = \frac{\sqrt{3}+1}{2\sqrt{3}} \qquad \text{and} \qquad N_1(p_2) = N_2(p_1) = \frac{\sqrt{3}-1}{2\sqrt{3}}.$$

Therefore, from equation (3.9) we have, integrating over Ω_e,

$$I_2[N_1^2] = I_2[N_2^2] = \tfrac{1}{2} I_2[N_1 N_2] = \frac{h}{3}$$

and, since $N_1' = -\frac{1}{h} = -N_2'$, we get

$$I_2[N_1'^2] = I_2[N_2'^2] = -I_2[N_1'N_2'] = \frac{1}{h}$$

and

$$I_2[N_1'N_1] = I_2[N_1'N_2] = -I_2[N_2'N_1] = -I_2[N_2'N_2] = -\frac{1}{2}.$$

Thus

$$\begin{aligned}
d^{-1}\,\|\varepsilon(x_h^{(e)})\|^2 &= d^{-1}\,I_2[(u_h' + \beta\, w_h)^2] \\
&= d^{-1}\,I_2[(\textstyle\sum_{i=1}^2 u_i N_i')^2 + 2\beta \sum_{i=1}^2 \sum_{j=1}^2 u_i w_j N_i' N_j + \beta^2 (\sum_{j=1}^2 w_j N_j)^2] \\
&= d^{-1}\,\frac{(u_2-u_1)^2}{h^2} h + 2\beta d^{-1}\,\frac{(u_2-u_1)}{h}\frac{(w_1+w_2)}{2} h \\
&\quad + d^{-1}\,\beta^2\,\frac{(w_1+w_2)^2}{h^2} h^3 + \frac{d^{-1}\beta^2}{12}\,\frac{(w_2-w_1)^2}{h^2} h^3 \\
&= d^{-1}\left(\frac{u_2-u_1}{h} + \beta\,\frac{w_1+w_2}{2}\right)^2 h + \frac{d^{-1}\beta^2}{12}\,\frac{(w_2-w_1)^2}{h^2} h^3.
\end{aligned}$$

Therefore as $d \to 0$, the two constraints that emerge in the limit are

$$\frac{u_2-u_1}{h} + \beta\,\frac{w_1+w_2}{2} = 0 \qquad \textit{and} \qquad \frac{w_2-w_1}{h} = 0\,.$$

These are the discretized equivalents of the true inextensional strain condition $u' + \beta w = 0$ and the spurious constraint $w' = 0$. Hence, over each element Ω_e, $w = c$ for some constant c which, by application of the boundary conditions, is zero and therefore $w = u = 0$. It is this spurious constraint that causes membrane (in-plane) locking and arises due to the difference in order of the basis functions for u_h' and w_h. Applying exact integration to the discretized shear term gives

$$\begin{aligned}
d^{-1}\,\|\gamma(x_h^{(e)})\|^2 &= I_2[(\,w_h' - \beta\, u_h - \phi_h\,)^2] \\
&= I_2[(\,w_i N_i' - \beta u_i N_i - \phi_i N_i\,)^2] \\
&\simeq d^{-1}\left(\frac{(w_2-w_1)}{h} - \beta\frac{u_1+u_2}{2} - \frac{\phi_1+\phi_2}{2}\right)^2 h \\
&\quad + \frac{d^{-1}h^3}{12}\left(\beta\frac{u_2-u_1}{h} + \frac{\phi_2-\phi_1}{h}\right)^2.
\end{aligned}$$

Therefore, the two constraints that emerge in limit $d \to 0$ are

$$\frac{(w_2 - w_1)}{h} - \beta\frac{u_1 + u_2}{2} - \frac{\phi_1 + \phi_2}{2} = 0 \qquad \text{and} \qquad \beta\frac{u_2 - u_1}{h} + \frac{\phi_2 - \phi_1}{h} = 0.$$

These are the discrete equivalents of the true Kirchhoff constraint $w' - \beta\, u - \phi = 0$ and the spurious constraint $\beta u' + \phi' = 0$ which causes shear locking.

Note

1. The true and spurious constraints, due to the shear and axial strains, are multiplied by the terms h and h^3 respectively. Hence, as the number of finite elements increase, $h^3 \to 0$ faster than h, thus relaxing the spurious constraints.

2. As the arch gets shallower the β^2 term (that is, the spurious constraint of the axial strain) tends to zero, thus neutralising the locking effects of the spurious constraint.

Applying reduced integration to the membrane term, over the element Ω_e, would require the use of 1-point Gaussian quadrature for which the weight and abscissa are given by $w = 2$ and $a = 0$ respectively. From these values we obtain

$$I_1[N_1^2] = I_1[N_2^2] = I_1[N_1 N_2] = \frac{h}{4}$$

and

$$I_1[N_1'^2] = I_1[N_2^2] = -I_1[N_1' N_2'] = \frac{1}{h}.$$

Hence,

$$\begin{aligned} d^{-1}\, I_1[(\varepsilon(x_h^{(e)}))^2] &= d^{-1}\,\frac{(u_2 - u_1)^2}{h^2}h + 2\beta d^{-1}\,\frac{(u_2 - u_1)}{h}\frac{(w_1 + w_2)}{2}h \\ &\quad + d^{-1}\,\beta^2\,\frac{(w_1 + w_2)^2}{h^2}h \\ &= d^{-1}\left(\frac{u_2 - u_1}{h} + \beta\,\frac{w_1 + w_2}{2}\right)^2 h. \end{aligned}$$

Therefore as $d \to 0$ the only constraint that emerges is the true inextensibility constraint.

Similarily, applying 1-point Gaussian quadrature to the discrete shear term leads to

$$d^{-1} I_1[\gamma(x_h^{(e)})] = d^{-1} \left(\frac{(w_2 - w_1)}{h} - \beta \frac{u_1 + u_2}{2} - \frac{\phi_1 + \phi_2}{2} \right)^2 h,$$

which produces only the true Kirchhoff constraint in the penalty limit.

Existence and Uniqueness

We now wish to identify the stability and convergence of the approximation scheme **R** by showing its equivalence to the discrete mixed problem $\mathbf{M}_h$. We make use of the procedure adopted by Arnold [13] and in order to do so propose the following:

Proposition 3.2 *For any* $f_h, g_h \in P_r^h \qquad \langle \pi_{r-1} f_h, g_h \rangle = \langle f_h, g_h \rangle_r.$

Proof: Let $I(f_h) \in P_{r-1}^h$ be the interpolate of f_h at the Gauss points. Then, for any $k_h \in P_{r-1}^h$, $I(f_h)k_h$ is a polynomial of degree $2r-2$. Therefore, since Gaussian integration of order r is exact for polynomials of degree $\leq 2r-1$, we have

$$\begin{aligned} \langle I(f_h), k_h \rangle &= \langle I(f_h), k_h \rangle_r \\ &= \langle f_h, k_h \rangle_r \qquad \text{(by def. of interpolate.)} \\ &= \langle f_h, k_h \rangle, \end{aligned}$$

since $f_h k_h$ is a polynomial of degree $2r-1$. So, by the definition of a projection operator,

$$I(f_h) = \pi_{r-1} f_h \qquad \text{(i)}$$

for any $f_h \in P_r^h$. Thus, for any $g_h \in P_r^h$

$$\begin{aligned} \langle \pi_{r-1} f_h, g_h \rangle &= \langle I(f_h), g_h \rangle \qquad \text{from (i)} \\ &= \langle I(f_h), g_h \rangle_r \qquad \text{(polynomial of deg. } 2r-1\text{).} \\ &= \langle f_h, g_h \rangle_r. \end{aligned}$$

■

We are now in a position to show the equivalence between the reduced standard problem and the discrete mixed problem.

Theorem 3.3 a. *The reduced integration formulation* **R** *of the standard problem is equivalent to the discrete mixed problem of finding* $\tilde{x}_h \in X^h$ *and* $\tilde{p}_h = (\tilde{\xi}_h, \tilde{\eta}_h) \in Q^h$ *such that*

$$\begin{aligned} \langle \tilde{\phi}'_h, \tilde{\psi}'_h \rangle + \langle \gamma(y_h), \tilde{\xi}_h \rangle + \langle \varepsilon(y_h), \tilde{\eta}_h \rangle &= F(y_h) \\ \langle \nu d^{-1}\gamma(\tilde{x}_h) - \tilde{\xi}_h, \kappa_h \rangle + \langle d^{-1}\varepsilon(\tilde{x}_h) - \tilde{\eta}_h, \lambda_h \rangle &= 0 \end{aligned} \tag{3.13}$$

for all $\tilde{y}_h \in X^h$ *and* $q_h = (\kappa_h, \lambda_h) \in Q^h$.

b. *Problem* **R** *or* $\mathbf{M}_h$ *has a unique solution* $\tilde{x}_h \in X^h$, $\tilde{p}^h \in Q^h$ *with*

$$\tilde{p}_h = (\tilde{\xi}_h, \tilde{\eta}_h) = d^{-1}(\pi_{r-1}\gamma(\tilde{x}_h), \pi_{r-1}\varepsilon(\tilde{x}_h).)$$

Furthermore, if $x \in (H^{r+1}(0,1))^3$, *then there exists a constant* $C > 0$, *independent of* ε *and* h, *such that*

$$|\tilde{x}_h - x|_1 \leq C h^r |x|_1 \tag{3.14}$$

Proof of a: Applying Proposition 3.2 to equation (3.12) gives

$$\langle \tilde{\phi}'_h, \psi'_h \rangle + \nu d^{-1}\langle \pi_{r-1}\gamma(\tilde{x}_h), \gamma(y_h) \rangle + d^{-1}\langle \pi_{r-1}\varepsilon(\tilde{x}_h), \varepsilon(y_h) \rangle = F(y_h)$$

for all $y_h \in X^h$. This implies that

$$\langle \tilde{\phi}'_h, \psi'_h \rangle + \nu d^{-1}\langle \tilde{\xi}_h, \gamma(y_h) \rangle + d^{-1}\langle \tilde{\eta}_h, \varepsilon(y_h) \rangle = F(y_h)$$

for all $y_h \in X^h$ iff

$$\begin{pmatrix} \tilde{\xi}_h \\ \tilde{\eta}_h \end{pmatrix} = \pi_{r-1} \begin{pmatrix} \nu d^{-1}\gamma(\tilde{x}_h) \\ d^{-1}\varepsilon(\tilde{x}_h) \end{pmatrix}, \tag{3.15}$$

that is, iff

$$\langle d^{-1}\gamma(\tilde{x}_h) - \tilde{\xi}_h\,,\, \kappa_h \rangle + \langle d^{-1}\varepsilon(\tilde{x}_h) - \tilde{\eta}_h\,,\, \lambda_h \rangle = 0$$

for all $(\kappa_h, \lambda_h) \in Q^h$. Since the procedure above is reversible, the converse also holds, thus completing the proof. Note that equations (3.13) are equivalent to equations (3.4) and (3.5).

Proof of b: The existence of a unique solution follows from theorem 3.1 while (3.14) follows from inequality (3.8) and interpolation theory. ∎

4 Numerical Results

Recall from theorem 3.3 that the error estimates for the mixed problem give

$$|U - U_h|_1 \leq ch^r |U|_1, \tag{4.1}$$

where U represents any one of the generalised displacements (ϕ, u or w) or the vector x. We expect, therefore, that the graph of numerical results of $\log |U - U_h|_1$ against $\log h$ would give a straight line of slope r, for sufficiently small h, if convergence occurs at the predicted rate.

In this section we present the results of numerical experiments undertaken with a view to verifying this error estimate for various situations. The aim is to compare results obtained by the standard formulation (with full integration) with those obtained by the mixed formulation. In the case of the latter we use the equivalent reduced integration formulation.

4.1 An Exact Solution

Since the aim is to obtain results of errors, that is differences between exact and approximate solutions, it is first of all necessary to construct an exact solution against which approximate solutions may be compared. In order to obtain an exact solution we eliminate the internal forces and generalised strains from equations (2.16), (2.17) and (2.18) to obtain a set of three simultaneous equations in the generalised strains. Writing $D \equiv \frac{d}{ds}$ we have, for $\nu = 1$,

$$(D^2 - \beta^2)u + 2\beta\, Dw - \beta\,\phi = -df_t\,, \tag{4.2}$$

$$-2\beta\, Du + (D^2 - \beta^2)w - D\phi = -df_n\,, \tag{4.3}$$

$$-\beta\, u + Dw + (dD^2 - 1)\phi = 0\,. \tag{4.4}$$

By taking $D(4.2) - \beta \times (4.3)$ we have

$$(D^2 + \beta^2)Du + \beta(D^2 + \beta^2)w = F \tag{4.5}$$

where $F = -d(Df_t - \beta f_n)$, while taking $-\frac{d^{-1}}{\beta} \times (4.2) + D(4.3) + (4.4)$ gives

$$(2\beta^2 + d^{-1})\, D^2 u + \beta(d^{-1} + \beta^2 - D^2)\, Dw = G\,, \tag{4.6}$$

where $G = d\beta\, Df_n - f_t$. Hence we have two equations involving u and w.

In order to eliminate one more variable, namely u, we integrate (4.6) over the interval $[0, s]$ to get

$$Du = \frac{H}{2\beta^2 + d^{-1}} - \frac{\beta(d^{-1} + \beta^2)}{(d^{-1} + 2\beta^2)}\, w + \frac{\beta}{(d^{-1} + 2\beta^2)}\, D^2 w \tag{4.7}$$

where $H(s) = \int_0^s G(t)dt + c$. Substitution of this result into (4.5) leads to the equation

$$(D^2 + \beta^2)^2 w = \frac{d^{-1} + 2\beta^2}{\beta}\, J \tag{4.8}$$

where $J = F - \frac{(D^2 + \beta^2)}{d^{-1} + 2\beta^2}\, H$. Hence we have a fourth order differential equation in w. The solution of the homogeneous equation

$$(D^4 + 2\beta^2 D^2 + \beta^4)\, w_o = 0$$

$$\text{is} \qquad w_o(s) = A\cos\beta s + B\sin\beta s + Cs\cos\beta s + Ks\sin\beta s\,,$$

where A, B, C and K are constants. Hence the solution to (4.8) is given by $w = w_o + w_p$ where w_p is a particular solution of (4.8). We choose applied loads

$$f_t = 0 \quad \text{and} \quad f_n(s) = \sin\pi s \tag{4.9}$$

to get, upon substitution,

$$J(s) = \frac{\beta \sin\pi s}{d^{-1} + 2\beta^2}\left(1 + d\pi^2 + d\beta^2\right) - \frac{\beta^2 c}{d^{-1} + 2\beta^2}\,.$$

Substitution of this into (4.8) gives

$$(D^2 + \beta^2)^2 w = (1 + d\pi^2 + d\beta^2)\sin\pi s - \beta c$$

for which a particular solution is $w_p(s) = E \sin \pi s + b$, where

$$E = \frac{1 + d\pi^2 + d\beta^2}{(\pi^2 - \beta^2)^2} \quad \text{and} \quad b = -\frac{c}{\beta^3} .$$

Hence the solution of (4.8) is

$$w(s) = (A + Cs)\cos \beta s + (B + Ks)\sin \beta s + E \sin \pi s - \frac{c}{\beta^3}.$$

The boundary condition $w(0) = 0$ yields $c = A\beta^3$, and hence $b = -A$. Integrating equation (4.7) over the interval $[0, s]$ and applying the boundary condition $u(0) = 0$, we obtain

$$\begin{aligned} u(s) &= -\frac{d\beta}{\delta\pi}\cos \pi s - \frac{\beta}{\delta}(d^{-1} + \beta^2)\int_0^s w(t)dt + \frac{1}{\delta}\left(\beta D w|_0^s + cs + \frac{d\beta}{\pi}\right) \\ &= \left(B - \frac{Cd^{-1}}{\beta\delta} + Ks\right)\cos \beta s - \left(A + Cs + \frac{Kd^{-1}}{\beta\delta}\right)\sin \beta s \\ &\quad + A\beta s - B + \frac{Cd^{-1}}{\beta\delta} + \frac{1}{\gamma}(\cos \pi s - 1)\left(2d\beta\pi + \frac{\beta}{\pi}\right) \end{aligned}$$

where $\delta = d^{-1} + 2\beta^2$ and $\gamma = (\pi^2 - \beta^2)^2$.

Also, from equation (4.2) we have

$$\begin{aligned} \phi(s) &= \left(\frac{1}{\beta}D^2 - \beta\right)u + 2\,Dw \\ &= -A\,\beta^2 s + B\,\beta + C\,\frac{d^{-1}}{\delta}\,(2\cos \beta s - 1) + K\,\frac{2d^{-1}}{a}\sin \beta s \\ &\quad + \frac{1}{\gamma}\left[\frac{\beta^2}{\pi}(1 - \cos \pi s) + \pi(\cos \pi s + 2d\beta^2)\right] . \end{aligned}$$

The four remaining unknown constants can be determined by applying the four remaining boundary conditions

$$\phi(0) = \phi(1) = w(1) = u(1) = 0.$$

This leads to four equations which are linear for A, B, C and K. The details are messy, and therefore omitted.

4.2 A Finite Element Program

The program ARCH was written, in standard Fortran 77, to test the error estimate of equation (4.1). A large amount of literature exists on the theory of the finite element method, for example Reddy [11] ,the four volumes of Oden *et al* [4] and Ciarlet [6], and on the construction of efficient finite element programs. (See Burnett [3] for a comprehensive reference of books on finite element programming). The basic structure of the program was based on the BEAM program of Hinton and Owen [8] and extensive use was made of the books by Burnett [3] and Akin [1].

In this section we formulate the stiffness matrix and force vector relating to the discrete standard problem and then give a brief description of the program noting, in particular, those areas which are unique to the program.

Stiffness Matrix and Force Vector

Recall from the Galerkin method that we can define our solution x_h, to the approximate standard formulation S_h by

$$x_h = \sum_{i=1}^{n} x_i N_i \ ,$$

where N_i are the basis functions spanning the subspace X^h of X. Hence we have from equation (3.3) of problem S_h that for any $y_h = \sum_{j=1}^{n} y_j N_j \in X^h$

$$\begin{aligned} & B_d(x_h, y_h) &&= F(y_h) \\ \Rightarrow \quad & B_d(\sum_{i=1}^{n} x_i N_i \, , \sum_{j=1}^{n} y_j N_j) &&= F(\sum_{j=1}^{n} y_j N_j) \\ \Rightarrow \quad & \sum_{i=1}^{n} x_i \, B_d(N_i, N_j)\, y_j &&= F(N_j)\, y_j \qquad \text{for } j = 1, \ldots, n \end{aligned}$$

$$\Rightarrow \qquad \sum_{i=1}^{n} x_i \underbrace{B_d(N_i, N_j)}_{K_{ij}} = \underbrace{F(N_j)}_{F_j} \qquad (j = 1, \ldots, n) \tag{4.10}$$

since $y_h \in X^h$ is arbitrary. The symmetric matrix $K_{ij} \equiv B_d(N_i, N_j)$ is the global stiffness matrix while $F_j \equiv F(N_j)$ is the global force vector.

Thus we have reduced the problem to one of solving the set of simultaneous linear equations

$$\sum_{i=1}^{n} K_{ij}\, x_i = F_j \ , \ j = 1, \ldots, n \ . \tag{4.11}$$

Once these equations are solved, we can obtain the approximate solution x_h from equation (4.11). Continuing with this analysis we note by definition of the bilinear form that

$$B_d(N_i N_j) \equiv K_{ij} = R_{ij} + \nu d^{-1} S_{ij} + d^{-1} Q_{ij} \tag{4.12}$$

where, denoting $\int_0^1 ds$ by $\int_\Omega$, we have

$$R_{ij} \equiv \langle N_i', N_j' \rangle = \begin{pmatrix} \int_\Omega N_i' N_j' & 0 & 0 \\ 0 & 0 & 0 \\ 0 & 0 & 0 \end{pmatrix},$$

$$S_{ij} \equiv \langle \gamma(N_i), \gamma(N_j) \rangle = \begin{pmatrix} \int_\Omega N_i N_j & \beta \int_\Omega N_i N_j & -\int_\Omega N_i N_j' \\ \beta \int_\Omega N_i N_j & -\beta^2 \int_\Omega N_i N_j & -\beta \int_\Omega N_i N_j' \\ -\int_\Omega N_i' N_j & -\beta \int_\Omega N_i' N_j & \int_\Omega N_i' N_j' \end{pmatrix},$$

and

$$Q_{ij} \equiv \langle \varepsilon(N_i), \varepsilon(N_j) \rangle = \begin{pmatrix} 0 & 0 & 0 \\ 0 & \int_\Omega N_i' N_j' & \beta \int_\Omega N_i' N_j \\ 0 & \beta \int_\Omega N_i N_j' & \beta^2 \int_\Omega N_i N_j \end{pmatrix}.$$

The stiffness matrix is separated as in equation (4.12) so that reduced integration may be selectively applied to the shear and axial terms.

Using the applied loads chosen in (4.9), the force vector is given by

$$F_j = \begin{pmatrix} 0 \\ 0 \\ N_j \sin \pi s \end{pmatrix}.$$

The Program Structure

Besides error estimates, the main aims when constructing this program were minimal compilation time and memory storage so that the program could be run efficiently on a standard personal computer.

Lagrangian polynomials are used as basis functions which for linear elements are given by

$$N_1(s) = \frac{s_2 - s}{s_2 - s_1} \quad \text{and} \quad N_2(s) = \frac{s - s_1}{s_2 - s_1},$$

while for quadratic elements they are

$$N_1 = \frac{(s - s_2)(s - s_3)}{(s_1 - s_2)(s_1 - s_3)}, \quad N_2 = \frac{(s - s_1)(s - s_3)}{(s_2 - s_1)(s_2 - s_3)} \quad \text{and} \quad N_3 = \frac{(s - s_1)(s - s_2)}{(s_3 - s_1)(s_3 - s_2)}.$$

Due to the uniformity of the arch geometry and material properties, different mesh size lengths are not necessary. Hence uniform meshes were used, thus eliminating the need for a master element and its associated complications.

The stiffness matrix values are stored using the bandwidth method of storage which, for this particular problem, is just as efficient as the skyline method. In an attempt to minimise the size of the program the stiffness matrix elements are calculated, instead of being stored as individual functions as is normally the practice ([3] [8]).

Figure 6 gives the structure of the main subroutines of program ARCH. Each of these subroutines uses one or more subroutines (or functions) in order to perform its task. From an efficiency point of view, this modular form of programming is essential as it allows for the repeated use of certain subroutines (for example the Gaussian quadrature subroutine) by various parts of the program. We now proceed to give a brief description of the subroutines listed in figure 6.

DATA This subroutine reads the following initial data from a data file:

The initial and final number of elements used for the finite element approximation.

The number of nodes per element implying the use of either linear or quadratic basis functions.

The number of Gauss points for each of the rotational, shear and axial terms.

The essential boundary conditions of the problem.

The values of the constants d, β and ν.

FDATA The following data is calculated for use in various parts of the program.

The number of nodes and the maximum sizes for the various arrays used in the assembly and storage routines.

The connectivity between the nodes and the elements, which is mainly required in the bandwidth storage scheme.

The coordinates of the nodal points (which are an equal distance apart).

ASSEMB This is the main assembly routine for the global stiffness matrix and force vector. In this subroutine, the values of the stiffness matrix and the force vector are calculated and stored. The matrices Q_{ij}, R_{ij} and S_{ij} (described earlier in this section) are calculated separately and then added together to form the global stiffness matrix K_{ij}. Hence reduced or exact integration may be applied to each term as required. Note that eight point gaussian quadrature is used to calculate the integrals involved in the force vector.

GREDUC and BAKSUB The main function of these sbroutines is to find n unknowns from n simultaneous equations using Gauss reduction. In particular, the nodal values are calculated from the stiffness matrix and force vector. Subroutine GREDUC applies

Gauss reduction to the augmented matrix while BAKSUB is used to calculate the unknowns from the Gauss reduced matrix.

CONSTS The constants A, B, C and K contain the thickness parameter d and therefore have to be calculated for each run of the program. The gauss reduction and back-substitution routines of GREDUC and BAKSUB are used to calculate these four constants from the four equations mentioned in subsection 4.1. The integrals contained in the equations are solved using eight point Gaussian quadrature.

RESULT This is an optional subroutine which displays the error between the exact nodal point values and their respective finite element approximations, when using INELM number of elements for the approximation.

VEROR The approximate solutions ϕ_h, u_h and w_h, associated with the INELM number of elements, are calculated. The log error of equation (4.1) is then calculated and stored, along with the log of the associated mesh-size parameter.

OUTERR This subroutine prints out the values of the log error and the log h, associated with the INELM number of elements, into an output file for graphical plotting. Only those points which are a certain pre-determined set length apart are printed, so as to avoid a clustering of points, in the graphical plot, as the mesh size gets smaller.

4.3 Computed Error Estimates

We now give the error estimates of equation (4.1) produced by the program ARCH. The program has been run on a VAX mainframe, using the VAX-Fortran compiler, and on a standard IBM-compatible personal computer, using a Watcom Fortran 77 compiler. The results of this section were run on the VAX mainframe computer.

We test the theory for both a shallow arch for which $\beta = 1$, and a complete ring fixed at one

point, for which $\beta = 2\pi$. The numerical results are intended to illustrate the behaviour of the discrete standard formulation when exact or selective reduced integration is used for varying thicknesses of the arch. For large values of the parameter d, we expect the predicted rates of convergence, according to equation (4.1), for both full and selective reduced integration. For small values of d however, we expect poor results with full integration (due to locking) but not with reduced integration. All of the graphs show plots of $\log |U - U_h|_1$ against $\log h$ where U is the rotation ϕ, tangential displacement u or normal displacement w. We omit the result for the error in the vector x as it simply mimics the behaviour found for individual components.

Figures 7-12 show results for a shallow arch, for which $\beta = 1$, with approximation by linear and quadratic elements. Figures 7 and 8 give results for a relatively thick arch with $d = 10^{-1}$. As expected, there was no distinguishable difference between results obtained using exact and reduced integration, and furthermore convergence was at the predicted rates.

Figures 9 and 10 show results for the case in which d is small, viz. $d = 10^{-6}$, for linear elements, while Figures 11 and 12 show results for the same value of d, but using quadratic elements. The results using exact integration are given in Figures 9 and 11; for linear elements there is a distinct lack of convergence while for quadratic elements the rate of convergence is evidently satisfactory, at least for sufficiently small values of h. The results using reduced integration, shown in Figures 10 and 12, give in both the linear and quadratic cases convergence at the predicted rates.

Figures 13–18 repeat the previous set of numerical results, this time for the full ring, with $\beta = 2\pi$. All of the results bear the same qualitative similarities to those for the case in which $\beta = 1$. Worth mentioning is the lack of convergence, in the case of linear elements when using full integration, and convergence at the predicted rate for reduced integration.

In Figures 17 and 18 the results for quadratic elements parallel those given earlier for the shallow arch. Here, in contrast to the linear case, exact integration gives good results for sufficiently small values of h, though the results for reduced integration show convergence at the predicted rate even for relatively small numbers of elements.

Finally, by using full integration on the axial term while underintegrating the shear term, we show in Figures 19 and 20 that, as the arch gets shallower , the possibility of membrane locking is minimised through the presence of the small term β^2 in the membrane term. Figure 19 shows that membrane locking is already reasonably minimised for the shallow arch, with $\beta = 1$, while almost non-existent for a very shallow arch with $\beta = 0.1$.

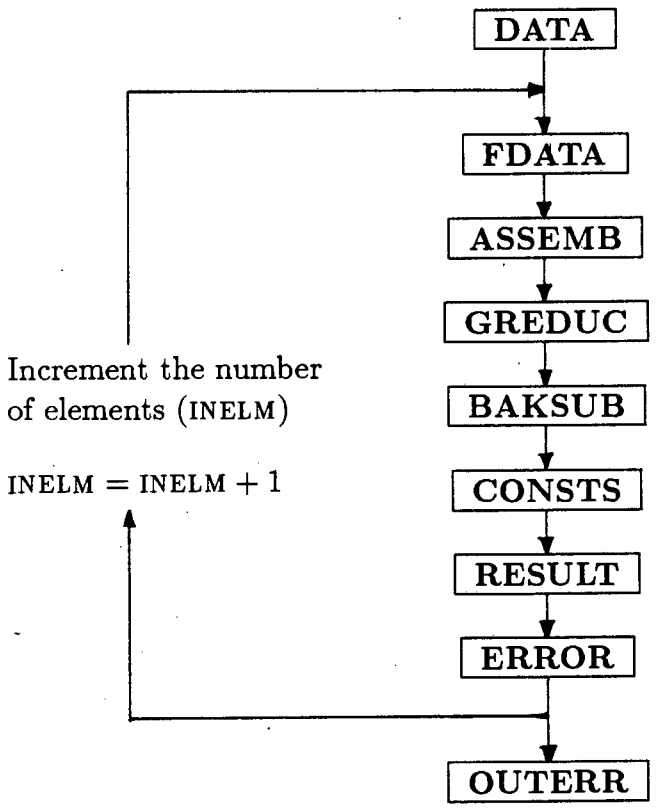

Figure 6: Basic structure of program ARCH listing the main subroutines.

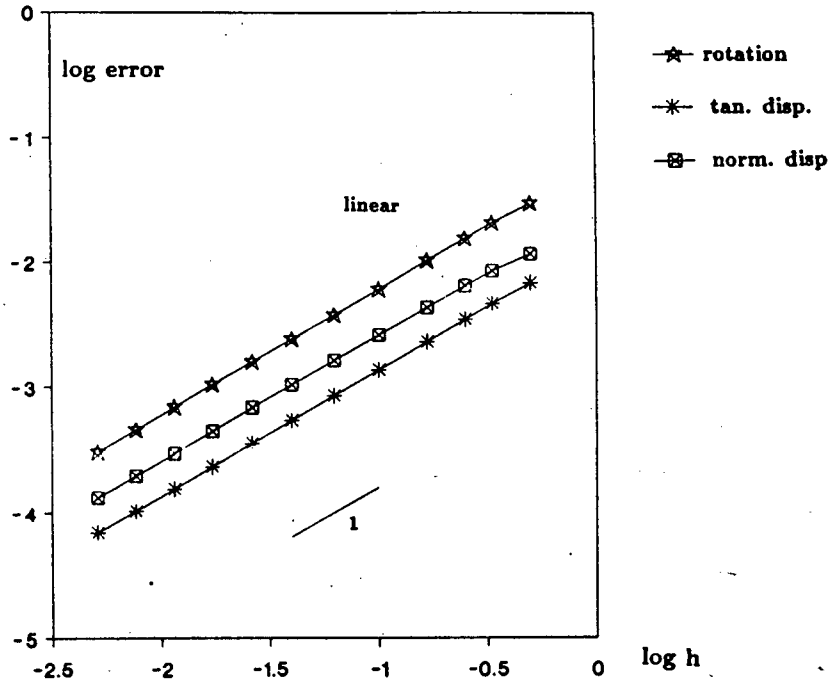

Figure 7: Log error vs log h for $\beta = 1$, $d = 10^{-1}$, linear elements, using exact or reduced integration.

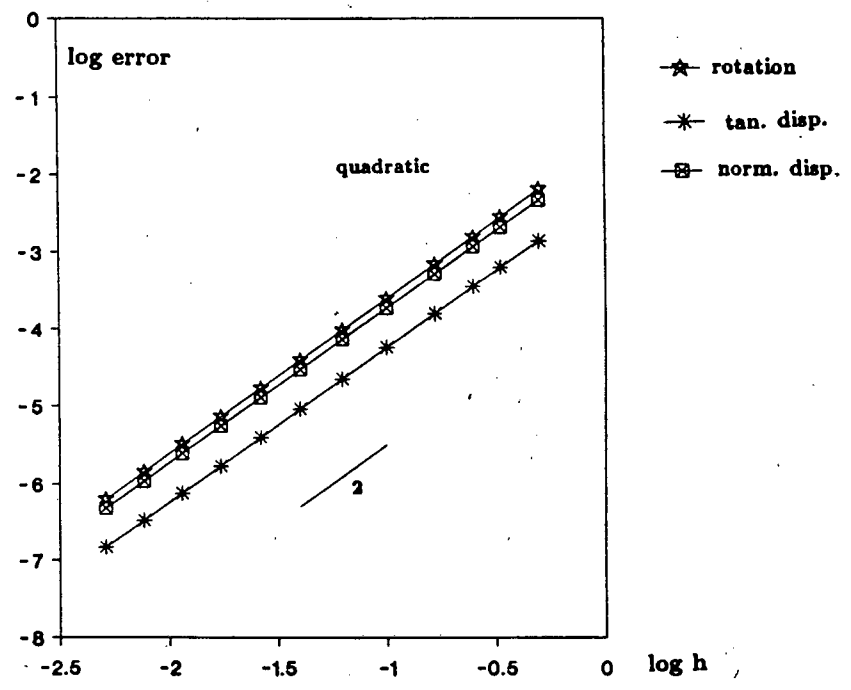

Figure 8: Log error vs log h for $\beta = 1$, $d = 10^{-1}$, quadratic elements, using exact or reduced integration.

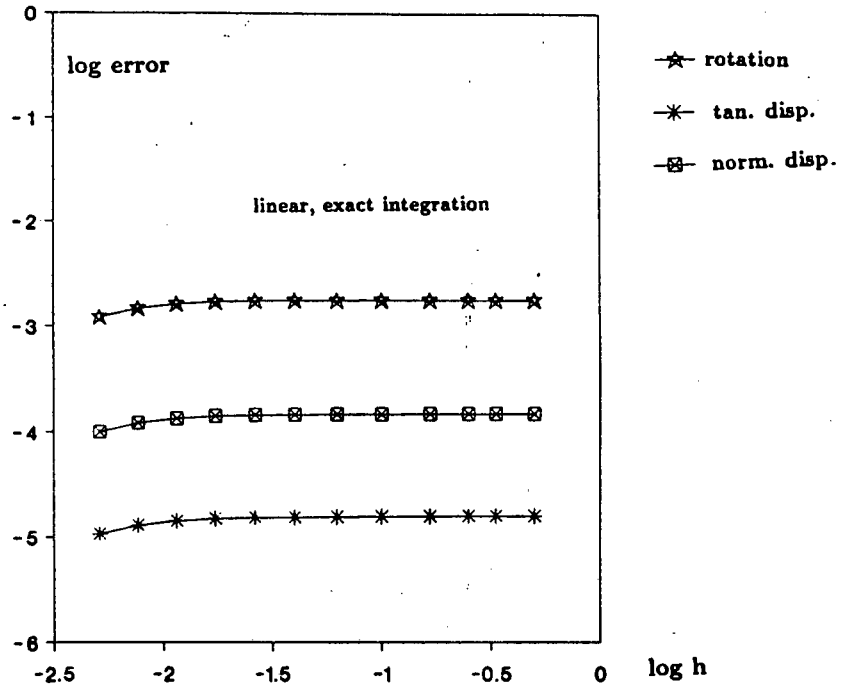

Figure 9: Log error vs log h for $\beta = 1$, $d = 10^{-6}$, linear elements, using exact integration.

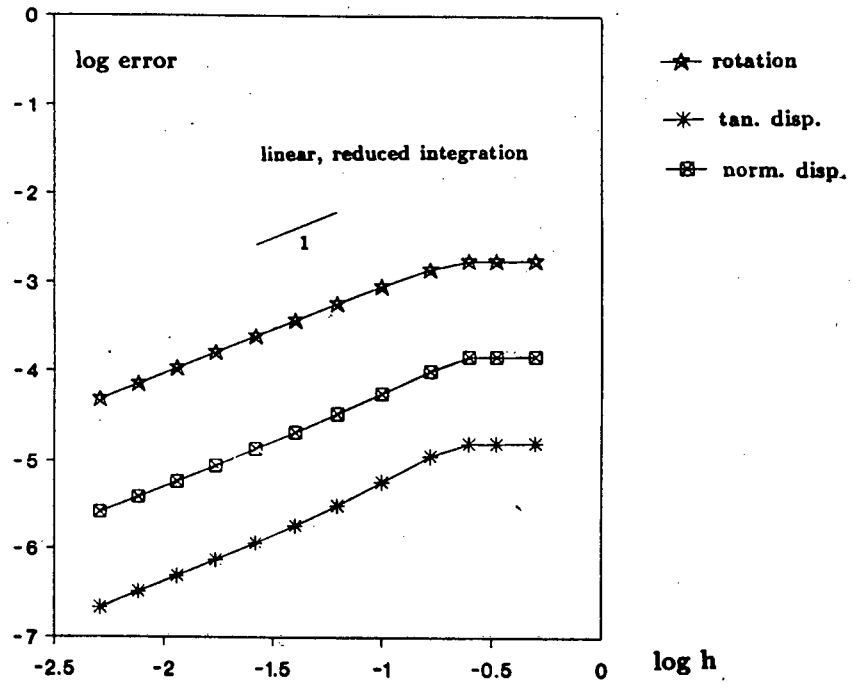

Figure 10: Log error vs log h for $\beta = 1$, $d = 10^{-6}$, linear elements, using reduced integration.

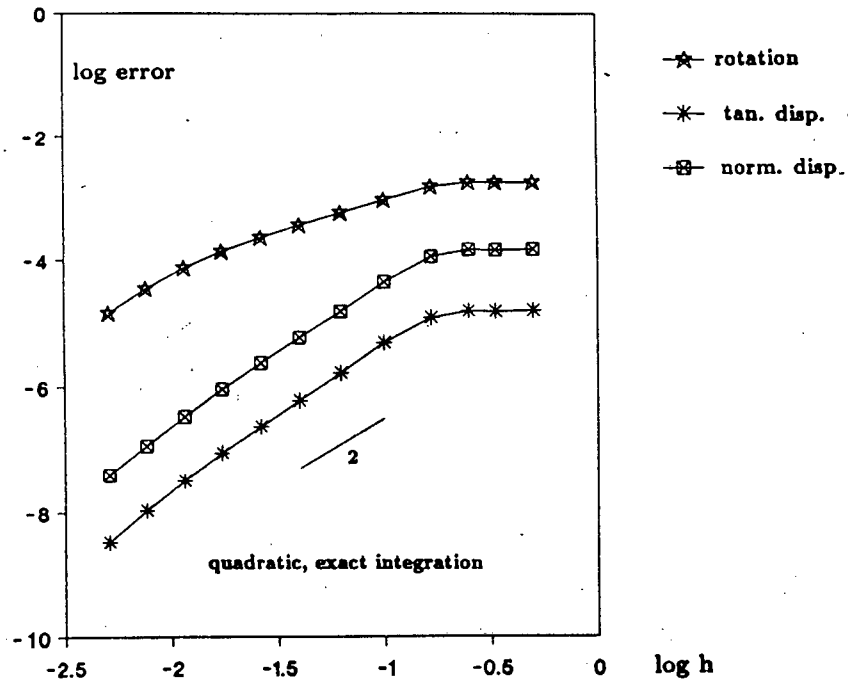

Figure 11: Log error vs log h for $\beta = 1$, $d = 10^{-6}$, quadratic elements, using exact integration.

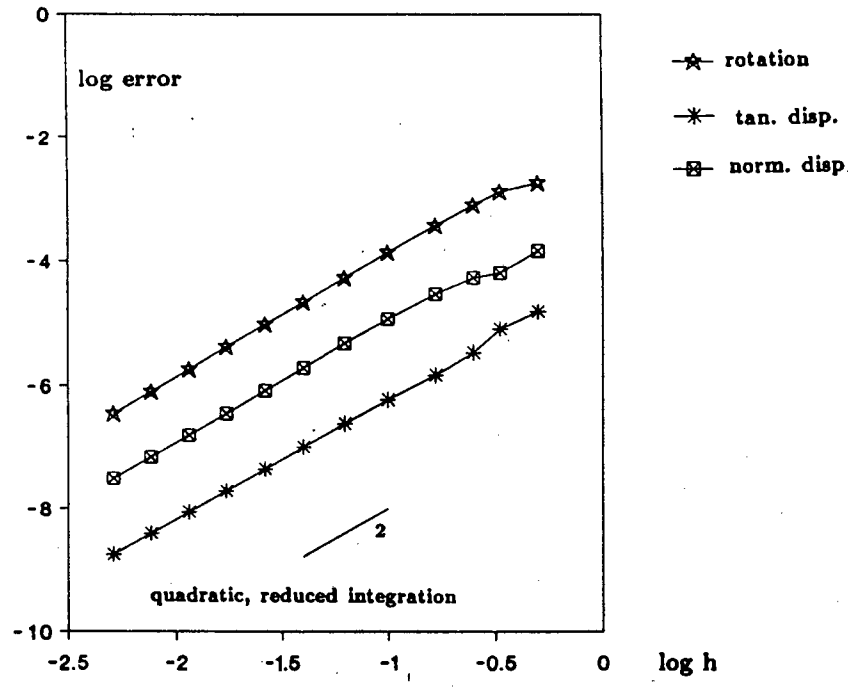

Figure 12: Log error vs log h for $\beta = 1$, $d = 10^{-6}$, quadratic elements, using reduced integration.

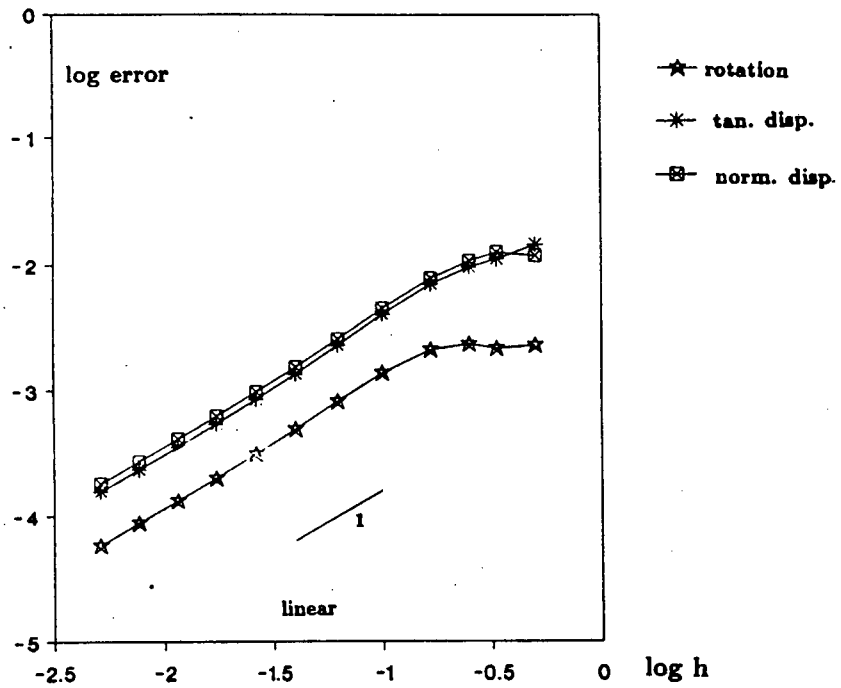

Figure 13: Log error vs log h for $\beta = 2\pi$, $d = 10^{-1}$, linear elements, using exact or reduced integration.

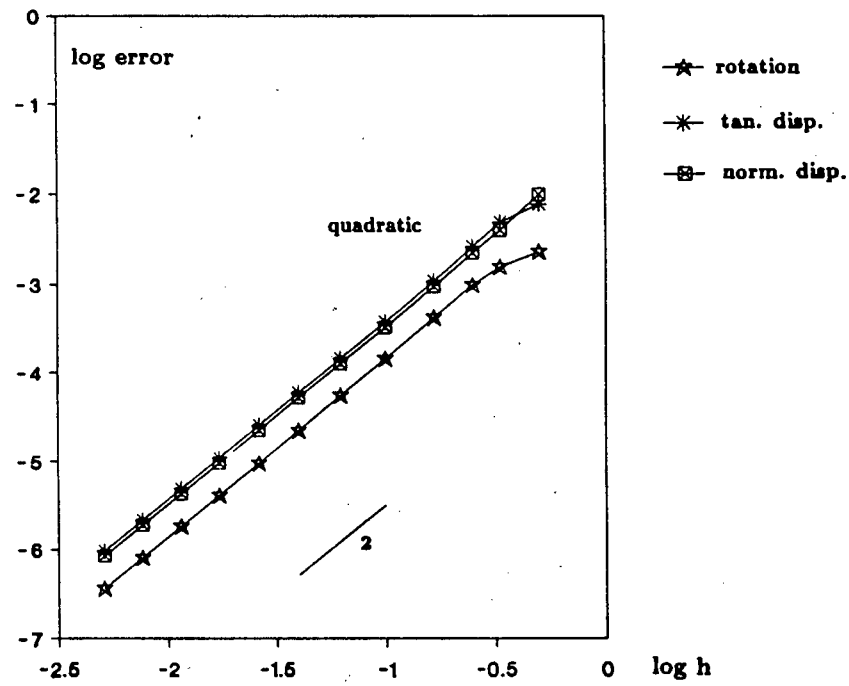

Figure 14: Log error vs log h for $\beta = 2\pi$, $d = 10^{-1}$, quadratic elements, using exact or reduced integration.

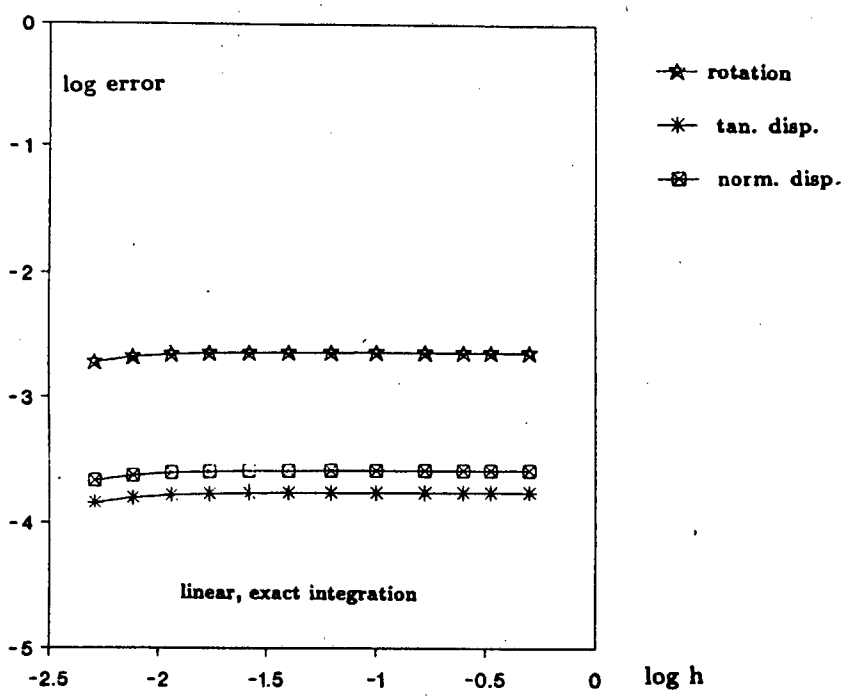

Figure 15: Log error vs log h for $\beta = 2\pi$, $d = 10^{-6}$, linear elements, using exact integration.

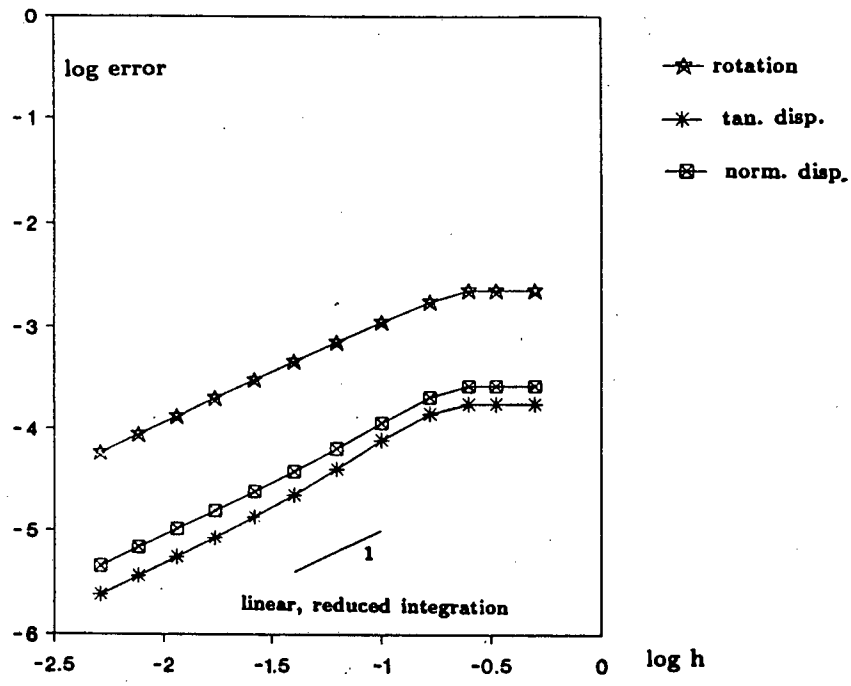

Figure 16: Log error vs log h for $\beta = 2\pi$, $d = 10^{-6}$, linear elements, using reduced integration.

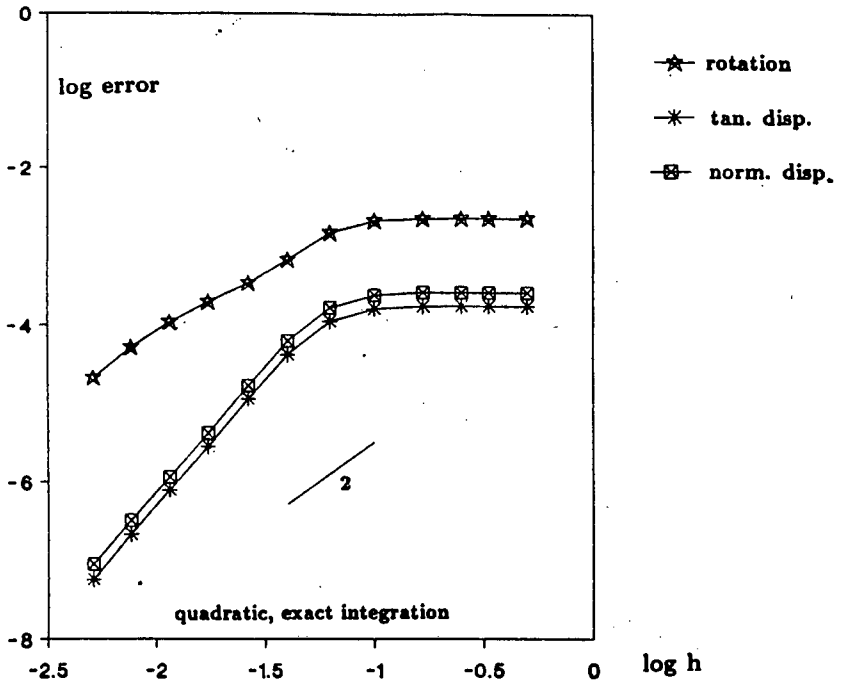

Figure 17: Log error vs log h for $\beta = 2\pi$, $d = 10^{-6}$, quadratic elements, using exact integration.

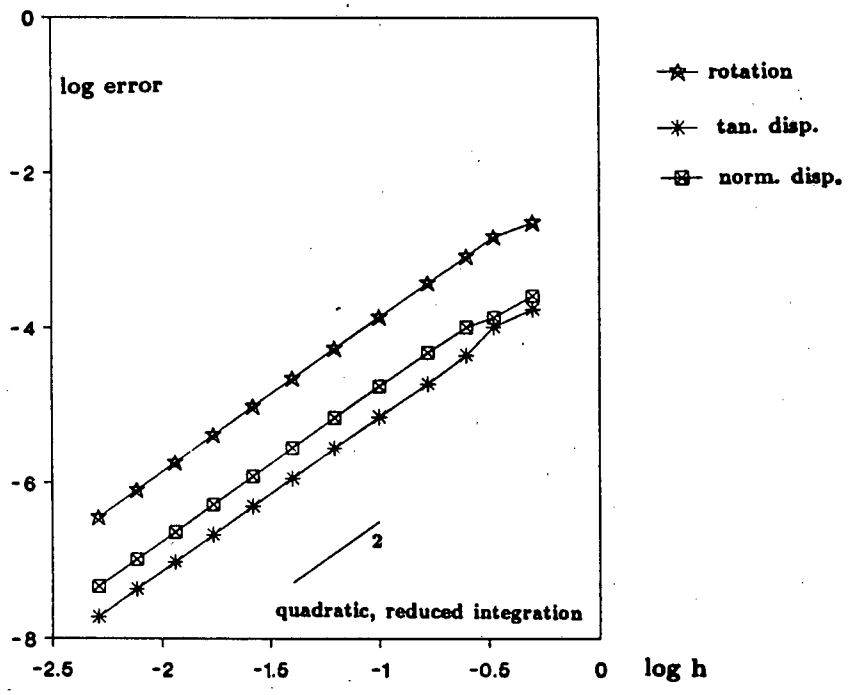

Figure 18: Log error vs log h for $\beta = 2\pi$, $d = 10^{-6}$, quadratic elements, using reduced integration.

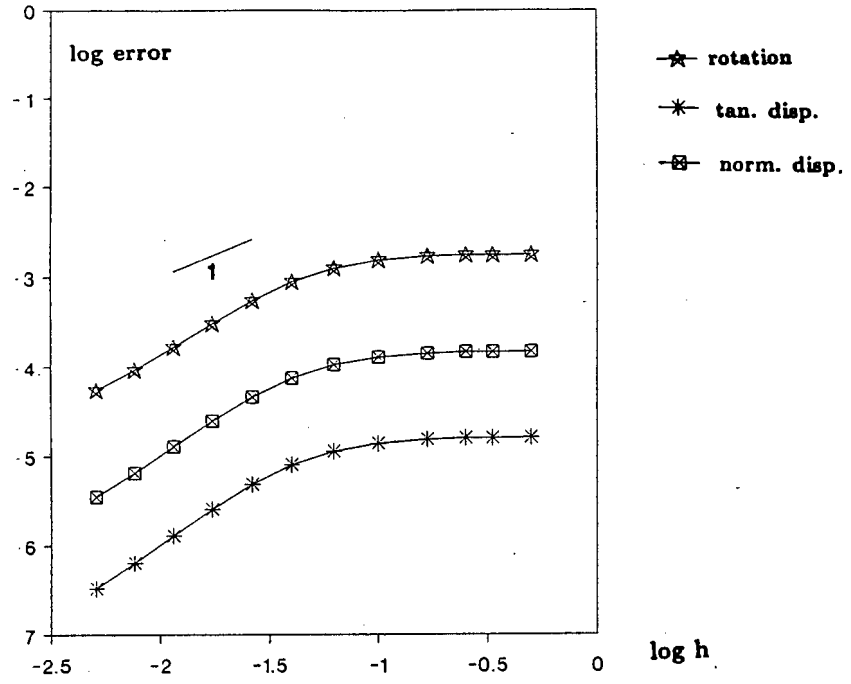

Figure 19: Log error vs log h for $\beta = 1$, $d = 10^{-6}$, linear elements, using reduced integration for the shear term and exact integration for the axial term.

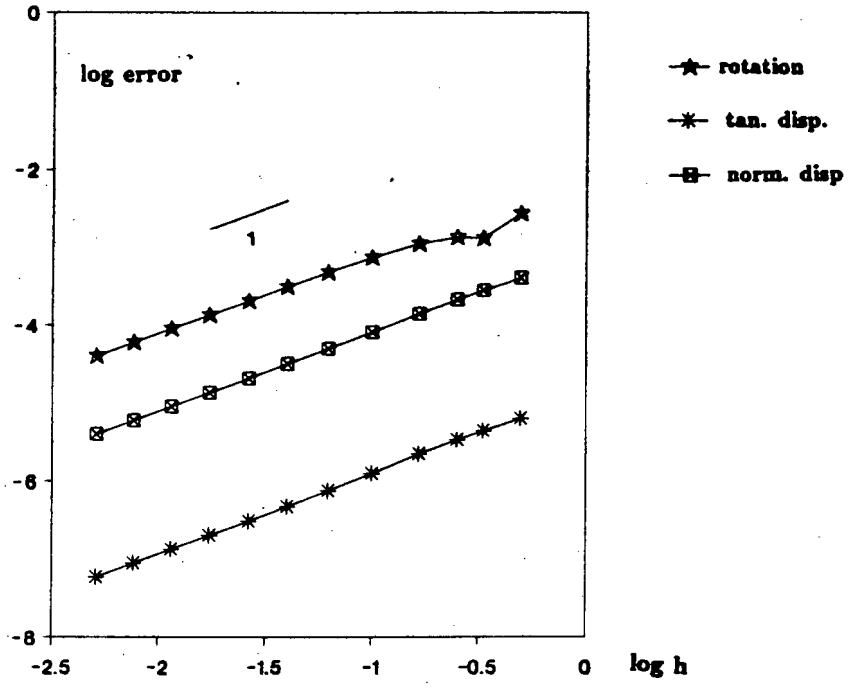

Figure 20: Log error vs log h for $\beta = 0.1$, $d = 10^{-6}$, linear elements, using reduced integration for the shear term and exact integration for the axial term.

A Geometrical formulation

In order to derive the equations (2.2) and (2.3) we note that

$$\hat{\mathbf{t}} = \frac{d\mathbf{r}}{d\bar{s}}. \tag{A.1}$$

This result can be obtained graphically, as illustrated in Figure A. Consider two position vectors $\mathbf{r}$ and $\mathbf{r} + d\mathbf{r}$ whose end points on the arch are an arc length $d\bar{s}$ apart. The difference $d\mathbf{r}$ is the chord joining these two points. In the limit, as $d\bar{s} \to 0$, the direction of the chord takes the direction of the tangent at the point defined by $\mathbf{r}(\bar{s})$.
Also, since $|d\mathbf{r}| = d\bar{s}$, $\frac{d\mathbf{r}}{d\bar{s}}$ is a unit vector.

Now note the tangent vectors $\hat{\mathbf{t}}$ and $\hat{\mathbf{t}} + d\hat{\mathbf{t}}$ defined for points $\bar{s}$ and $\bar{s} + d\bar{s}$ in Figure A(b). Dividing by $d\bar{s}$ and letting $d\bar{s} \to 0$, it can be seen that $\frac{d\hat{\mathbf{t}}}{d\bar{s}}$ is normal to $\hat{\mathbf{t}}$. Hence we can set

$$\hat{\mathbf{n}} = \rho \frac{d\hat{\mathbf{t}}}{d\bar{s}} \tag{A.2}$$

for some value ρ. Since $\hat{\mathbf{n}}$ is a unit vector we set

$$\frac{1}{|\rho|} = |\frac{d\hat{\mathbf{t}}}{d\bar{s}}|.$$

Also, in order to ensure that $\hat{\mathbf{n}}$ is in the right direction, we make ρ positive if the curve is convex with respect to the origin O, and negative if concave.

From Figure A we can see that ρ is actually the *radius of curvature* of the arch. Let the normal to vectors $\hat{\mathbf{t}}$ and $\hat{\mathbf{t}} + d\hat{\mathbf{t}}$ intersect at point O' with an angle $d\theta$ between them. This angle $d\theta$ is also the angle between $\hat{\mathbf{t}} + d\hat{\mathbf{t}}$. Hence $d\theta = |d\hat{\mathbf{t}}|$ and $\frac{d\theta}{d\bar{s}} = |\frac{d\hat{\mathbf{t}}}{d\bar{s}}|$. But by definition of radian measure we know that $O'C = \frac{d\bar{s}}{d\rho}$ and hence $\rho = O'C$. So, since $|\rho| = R$ and the arch is convex with respect to the origin, we have

$$\frac{d\hat{\mathbf{t}}}{d\bar{s}} = -\frac{1}{R}\hat{\mathbf{n}}$$

To derive the other equation we introduce the relationship between the local and cartesian coordinates which, if the $\hat{\mathbf{t}}$ direction is inclined at an angle α to the $\hat{\mathbf{i}}$ direction (measured anticlockwise), is given by

$$\begin{aligned} \hat{\mathbf{t}} &= (\cos\alpha)\hat{\mathbf{i}} + (\sin\alpha)\hat{\mathbf{j}}\,, \\ \hat{\mathbf{n}} &= -(\sin\alpha)\hat{\mathbf{i}} + (\cos\alpha)\hat{\mathbf{j}}\,. \end{aligned} \tag{A.3}$$

Hence if

$$\mathbf{r} = r_x\hat{\mathbf{i}} + r_y\hat{\mathbf{j}} \tag{A.4}$$

we have

$$\hat{\mathbf{t}} = \frac{d\mathbf{r}}{d\bar{s}} = \frac{dr_x}{d\bar{s}}\hat{\mathbf{i}} + \frac{dr_y}{d\bar{s}}\hat{\mathbf{j}}\,. \tag{A.5}$$

Now

$$\hat{\mathbf{n}} = \rho\frac{d\hat{\mathbf{t}}}{d\bar{s}} = \rho\frac{d^2r_x}{d\bar{s}^2}\hat{\mathbf{i}} + \rho\frac{d^2r_y}{d\bar{s}^2}\hat{\mathbf{j}}\,. \tag{A.6}$$

However, comparing equations (A.2), (A.3) and (A.4)–(A.6), we see that

$$\frac{dr_x}{d\bar{s}} = \rho\frac{d^2r_y}{d\bar{s}^2}, \qquad \frac{dr_y}{d\bar{s}} = -\rho\frac{d^2r_x}{d\bar{s}^2}, \tag{A.7}$$

and

$$\hat{\mathbf{n}} = -\frac{dr_y}{d\bar{s}}\hat{\mathbf{i}} + \frac{dr_x}{d\bar{s}}\hat{\mathbf{j}}\,. \tag{A.8}$$

Therefore, from equation (A.8), using equations (A.7) and (A.3),

$$\begin{aligned} \frac{d\hat{\mathbf{n}}}{d\bar{s}} &= -\frac{d^2r_y}{d\bar{s}^2}\hat{\mathbf{i}} + \frac{d^2r_x}{d\bar{s}^2}\hat{\mathbf{j}} \\ &= -\frac{1}{\rho}\frac{dr_x}{d\bar{s}}\hat{\mathbf{i}} - \frac{1}{\rho}\frac{dr_y}{d\bar{s}}\hat{\mathbf{j}} \\ &= -\frac{1}{\rho}\hat{\mathbf{t}}\,. \end{aligned}$$

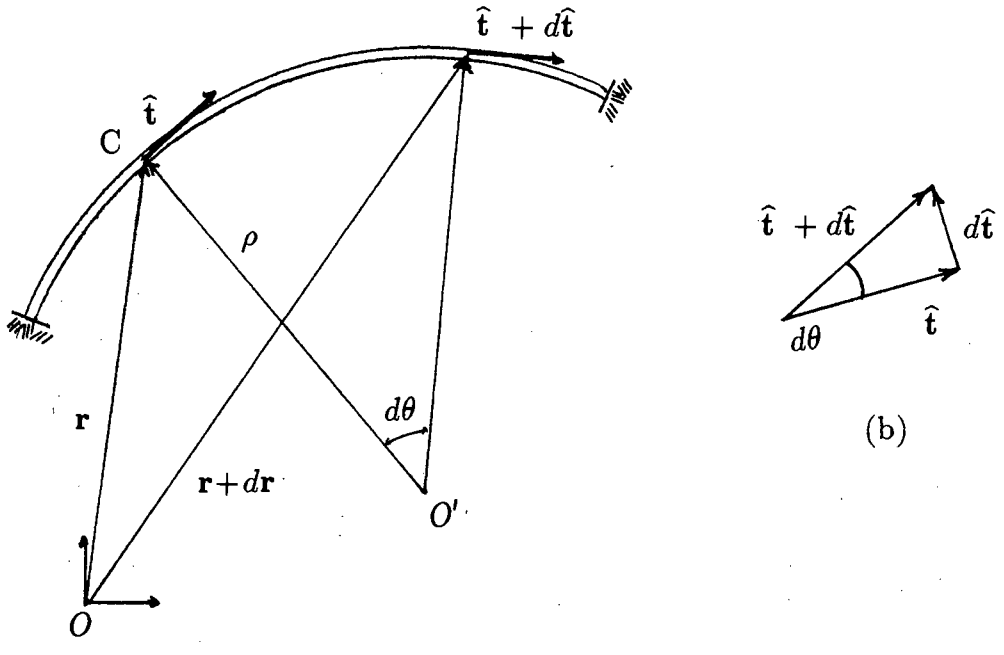

Figure 21: Directions of local basis vectors and their derivatives.

Acknowledgements

I am greatly indebted to the excellent supervision of Professor Dayanand Reddy; in particular for his inspiring knowledge, patient support, good humour and welcoming friendship. I would like to thank Professor Franco Brezzi, Dr. Donatella Marini and Professor Ray Ogden for their encouraging support and inspiration while on conference at the University of Cape Town. Many thanks to my close friend and colleague Archie Maurellis for all his support and assistance during the write- up of the thesis. I would also like to thank Robin Eve for his help in the finite element computation and Diane Loureiro for all her help and encouragement. Special thanks to my better half, Carol Booysen, for all her help, encouragement and loving support throughout the year. Finally I would like to thank the Foundation for Research and Development for making it financially possible for me to complete a masters degree.

References

[1] Akin, J.E.: Application and Implementation of Finite Element Methods. Academic Press (1982)

[2] Ashwell, D.G., Gallagher, R.H.: Finite Elements for Thin Shells and Curved Members. Wiley (1976)

[3] Burnett, D.S.: Finite Element Analysis : From Concepts to Applications. Addison Wesley (1987)

[4] Carey, G.F., Oden, J.T.: Finite Elements: A Second Course. **II** (1982)

[5] Cook, R.D.: Concepts and Applications of Finite Element Analysis. Prentice-Hall (1982)

[6] Ciarlet, P.G.: The Finite Element Method for Elliptic Problems. North-Holland (1978)

[7] Duvaut, G., Lions, J.L.: Inequalities in Mechanics and Physics. Springer and Verlag (1976)

[8] Hinton, E., Owen, D.R.J.: Finite Element Programming. Academic Press (1977)

[9] Kreyszig, E.: Introductory Functional Analysis with Applications. Wiley (1978)

[10] Martin, J.B., Reddy, B.D.: Structural Mechanics course notes. Dept. Civil Engineering, Univ. of Cape Town (1981)

[11] Reddy, B.D.: Functional Analysis and Boundary value problems: an introductory treatment. Longman & Wiley (1986)

[12] Zienkiewicz, O.C.: The finite element method. McGraw-Hill, London, 3rd ed., (1977)

[13] Arnold, D.N.: Discretization by finite elements of a model parameter-dependent problem. *Numer. Math.* **37**, 405–421 (1981)

[14] Ashwell, D.G., Sabir, A.B.: Limitations of certain curved finite elements when applied to arches. *Int. J. Mech. Sci.* **13**, 133–139 (1971)

[15] Babuška, I.: The finite element method with Lagrangian multipliers. *Numer. Math.* **20**, 179–192 (1973)

[16] Batoz J.L.: An explicit formulation for an efficient triangular plate-bending element. *Int. J. Numer. Meths. Eng.* **18**, 1077–1089 (1982)

[17] Batoz, J.L., Bathe, K.J., HO, L.W.: A study of three-node triangular plate bending elements. *Int. J. Numer. Meths. Eng.* **15**, 1771–1812 (1980)

[18] Brezzi, F.: On the existence, uniqueness and approximation of saddle-point problems arising from Lagrangian multipliers. *RAIRO Ser. Rouge Anal. Numér.* **8** 129–151 (1974)

[19] Brezzi, F.: Sur l'existence, unicité, et approximation de problèmes de point de selle. *C.R. Acad. Sci Paris Sér. A.* **278**, 839-842 (1974)

[20] Brezzi, F., Fortin, M.: Analysis of some low-order finite element schemes for Mindlin-Reissner plates. *Math. Comp.* **47**, 151-158 (1986)

[21] Dhatt G.:An efficient triangular shell element. *AIAA J.* **8**, 2100–2102 (1970)

[22] Dawe D.J.:High-order triangular finite element for shell analysis. *Int. J. Solids Struct.* **11**, 1097 (1975)

[23] Dvorkin, E.N., Oñate, E., Oliver, J.: On a non-linear formulation for curved Timoshenko beam elements considering large displacement/rotation increments. *Int. J. Numer. Meths. Eng.* **26**, 1597–1613 (1988)

[24] Ferguson, G.H., Clark, R.D., A variable thickness, curved beam and shell stiffening element with shear deformations. *Int. J. Numer. Meths. Eng.* **14**, 581–592 (1979)

[25] Franca, L.P., Hughes, T.J.R.: Two classes of mixed finite element methods. *Comput. Methods App. Mech. Eng.* **69**, 89–129 (1988)

[26] Kikuchi, F.: Accuracy of some finite element models for arch problems. *Comput. Methods App. Mech. Eng.* **35**, 315–345 (1982)

[27] Kikuchi, F.: On a finite element scheme based on the discrete Kirchhoff assumption. *Numer. Math.* **24**, 211–231 (1975)

[28] Loula, A.F.D., Hughes, T.J.R, Franca, L.P.: Petrov-Galerkin formulations of the Timoshenko beam problem. *Comput. Methods App. Mech. Eng.* **63**, 115–132 (1987)

[29] Loula, A.F.D., Franca, L.P., Hughes, T.J.R., Miranda, I.: Stability, convergence and accuracy of a new finite element method for the circular arch problem. *Comput. Methods App. Mech. Eng.* **63**, 281–303 (1987)

[30] Herrmann, L.R.: A bending analysis of plates. *Proc. Conf. Matrix Methods in Structural Mechanics* AFFDL-TR-66-80, 577 (1966)

[31] Hughes T.J.R., Taylor, R.L, Kanoknukulchai, W.: A simple and efficient finite element for plate bending. *Int. J. Numer. Meths. Eng.* **11**, 1529–1543 (1977)

[32] Malkus, D.S., Hughes, T.J.R.: Mixed finite element methods– reduced and selective integration techniques: a unification of concepts. *Comput. Methods Appl. Mech. Eng.* **15**, 63–81 (1978)

[33] Meck, H.R.: An accurate polynomial displacement function for finite ring elements. *Comp. Struct.* **11** 265–269 (1980)

[34] Noor, A.K., Greene, W.H., Hartley, S.J.: Nonlinear finite element analysis of curved beams. *Comput. Methods App. Mech. Eng.* **12**, 289–307 (1977)

[35] Noor, A.K., Peters, J.M.: Mixed models and reduced/selective integration displacement models for non-linear analysis of curved beams. *Int. J. Numer. Meths. Eng.* **17**, 615–631 (1981)

[36] Oden, J.K., Kikuchi, N., Song, Y.J.: Penalty-finite element methods for the analysis of Stokesian flows. *Comput. Methods Appl. Mech. Eng.* **31**, 297–329 (1982)

[37] Ortiz, M., Morris, G.R.: C^0 Finite element discretization of Kirchhoff's Equations of thin plate bending. *Int. J. Numer. Meths. Eng.* **26**, 1551–1566 (1988)

[38] Pian, T.H.H, Chen, D.P.: Alternative ways for formulation of hybrid stress elements. *Int. J. Numer. Meths. Eng.* **18**, 1679–1684 (1982)

[39] Prathap, G., Bhashyam G.R., : Reduced integration and the shear-flexible beam element. *Int. J. Numer. Meths. Eng.* **18**, 195–210 (1982)

[40] Prathap, G.: The curved beam/deep arch/finite ring element revisited. *Int. J. Numer. Meths. Eng.* **21**, 389–407 (1985)

[41] Reddy, B.D.: Convergence of mixed finite element approximations for the shallow arch problem. *Numer. Math.* **53**, 687–699 (1988)

[42] Stolarski, H., Belytschko, T.: Shear and memebrane locking in curved C^0 elements. *Comput. Methods Appl. Mech. Eng.* **41**, 279–296 (1983)

[43] Stolarski, H., Belytschko, T.: Membrane locking and reduced integration for curved elements. *ASME J. App. Mech.* **49**, 172–176 (1982)

[44] Saleeb, A.F., Chang, T.Y.: On the hybrid-mixed formulation of C^0 curved beam elements. *Comput. Methods Appl. Mech. Eng.* **60**, 95–121 (1987)

[45] Tessler, A., Hughes J.R.: An improved treatment of transverse shear in the Mindlin-type four-node quadrilateral element. *Comput. Methods Appl. Mech. Eng.* **39**, 311–335 (1983)

[46] Tessler, A., Spiridigliozzi, L.: Resolving membrane and shear locking phenomena in curved shear-deformable axisymmetric shell elements. *Int. J. Numer. Meths. Eng.* **26**, 1071–1086 (1988)

[47] Zienkiewicz, O.C., Hinton, E.: Reduced integration fuction smoothing and non-conformity in finite element analysis (with special reference to thick plates). *J. Franklin Inst.* **302** (5&6), 443-461 (1976)

[48] Zienkiewicz, O.C., Taylor, R.L., Too, J.M.: Reduced integration technique in general analysis of plates and shells. *Int. J. Numer. Meths. Eng.* **3**, 275–290 (1971)